Influence of Solar Activity Cycles on Earth's Climate

ESA ITT AO/1-4618/NL/AR

Task 2 – Identification of Relevant Data

WP 201 – Solar Output

Technical Note

F. Boberg*, H. Lundstedt, and P. Wintoft
Swedish Institute of Space Physics
*Now at University of Leicester and Danish Meteorological Institute

8 June 2005

Document status sheet

ISSUE	REVISION	DATE	REASON FOR CHANGE
0	0	March 22, 2005	First draft.
0	1	April 15, 2005	Minor corrections to Appendix and Tables 3 and 4.
0	2	May 27, 2005	Added information about the database access, Section 3.2.
0	3	8 June 2005	Corrections made according to comments from the meeting at ESTEC 30 May 2005. The major change is the addition of geomagnetic data (Section 2.2.2).

Summary

The retrieval of a large number of different measures of solar activity output is presented. The measures are divided into measured Solar Physical Quantities (SPQ) and indicators. SPQ include electromagnetic radiation, solar wind components, particle fluxes, and magnetic fields. Solar indicators include indices such as the sunspot number, flare index, coronal activity, and UV/EUV indices. Solar indicators also include proxies such as ^{14}C and ^{10}Be concentrations, but also solar activity lists of coronal mass ejections, flares, and proton events. The data are given as daily averages, with the exception of the solar wind parameters (hourly averages), the group sunspot number (monthly averages), early readings of the sunspot number (monthly and yearly averages), and ^{14}C and ^{10}Be proxies (resolution from 10 years and above). All data are stored at and electronically retrievable from the Swedish Institute of Space Physics.

Contents

1 Introduction **1**

2 Solar output data **2**

2.1 Measured solar physical quantities 2

2.2 Indicators 8

3 Database **19**

3.1 Data sources 19

3.2 ISAC database 19

4 Conclusion **25**

5 Appendix - ISAC data tables **28**

1 Introduction

The aim of WP 201 is to identify data that permit quantification of climate variability due to variations in solar activity. There exist many different measures of solar activity that can be divided into two main categories: physical quantities that can be used as input to climate models and indicators that first need to be interpreted.

Measurements of solar physical quantities have only been carried out during the last decades. We therefore need to construct longer times series from less physics-based indicators such as indices in order to be able to study the solar-climate coupling during longer periods. The advantage of an index such as the sunspot number is the long time period for which it has been calculated. Recent high quality solar images and magnetograms make it also possible to reconstruct time series of solar physical quantities for the period sunspots have been counted (*Fligge et al.*, 2000). Furthermore, using proxies such as ^{14}C and ^{10}Be concentrations have made it possible to extend the reconstructions of solar activity to over 10,000 years (*Usoskin et al.*, 2003). These proxies also make it possible to study non-anthropogenic climate changes. The interpretation of solar output indicators will be discussed in detail in WP 304.

A compilation of all literary references presented in this report is stored at the Swedish Institute of Space Physics. All solar data presented in this report, with the exception of the high-resolution magnetograms, is electronically stored at and retrievable from the Swedish Institute of Space Physics. Data plots in this report are colour coded. Yearly values are given in black, monthly values in red, daily values in blue, and hourly values in green.

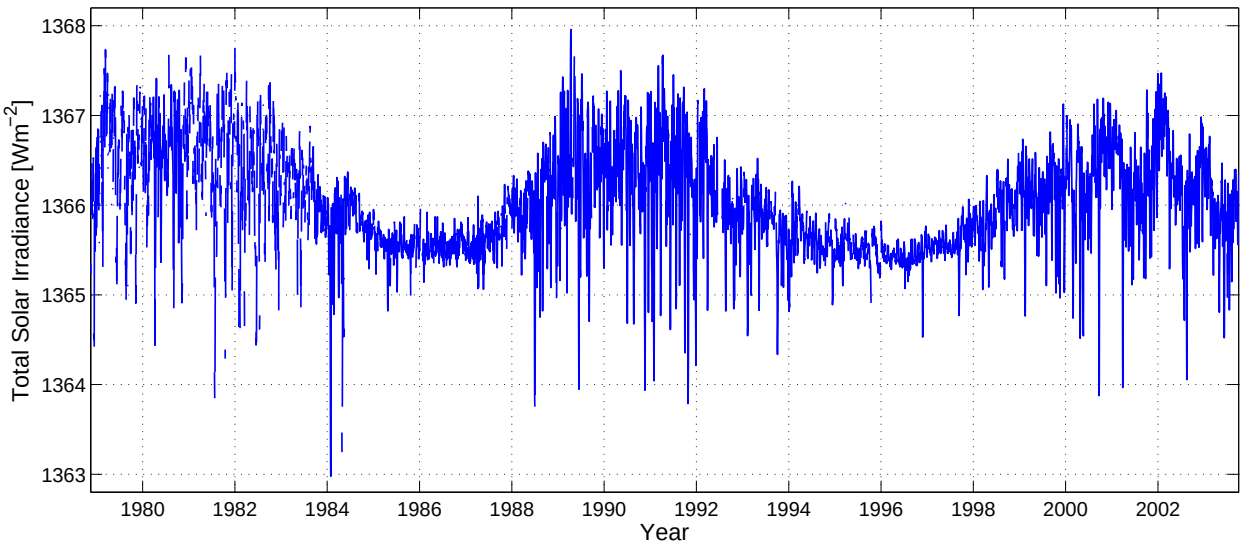

Figure 1: Composite plot of the total solar irradiance observed by 6 satellites: NIMBUS-7, SMM, ERBS, UARS, SOHO, and ACRIM-Sat.

2 Solar output data

The solar output data are divided into two sections. Section 2.1 describes the solar output with measured physical quantities. Section 2.2 describes the solar output using indicators. The indicators are further divided into indices, proxies, and lists.

2.1 Measured solar physical quantities

Total solar irradiance Total solar irradiance (TSI) describes the radiant energy emitted by the Sun over all wavelengths that falls each second on 1 square meter outside the Earth's atmosphere. This quantity is proportional to the "solar constant" observed earlier in this century. TSI monitoring begun in 1978 with a steady improvement in accuracy due to calibration procedures and comparison of data from different instruments. The TSI data available in this study, given in watts per square meter, is based on six different satellite observations covering the period 1978 to present (*Fröhlich and Lean*, 1998; *Lee III et al.*, 1995):

1. NIMBUS-7/HF (*Hoyt et al.*, 1992);
2. Solar Maximum Mission (SMM) Active Cavity Radiometer Irradiance Monitor Experiment (ACRIM I) (*Willson*, 1984);
3. The Earth Radiation Budget Satellite (ERBS) (*Lee III et al.*, 1987);
4. The Upper Atmospheric Research Satellite (UARS) Active Cavity Radiometer Irradiance Monitor II Experiment (ACRIM II) (*Willson*, 1994);

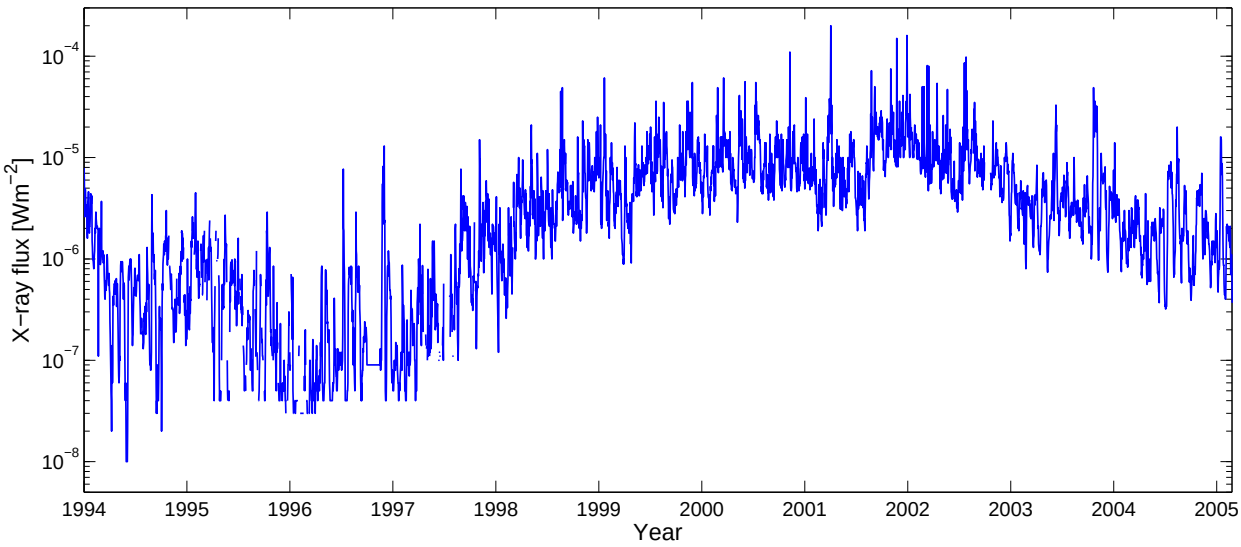

Figure 2: Daily values of X-ray background flux from 1994 onwards, obtained by GOES satellites.

Letter	Numeric value
A	10^{-8}
B	10^{-7}
C	10^{-6}
M	10^{-5}
X	10^{-4}

Table 1: Classification of X-ray flux using letters representing a value. The letter is followed by a number that is multiplied by the numeric value giving the actual flux intensity.

5. SOHO/VIRGO (*Fröhlich et al.*, 1997); and

6. ACRIM-Sat/ACRIM III (*Willson*, 2001).

The composite TSI time series, available at NOAA National Geophysical Data Center, is plotted in Figure 1, summarized in Table 4, and stored in the database as **noaa_tsi_comp** (see Table 3).

X-ray background flux X-ray background flux intensity has been calculated by Geostationary Operational Environmental Satellites (GOES) in the 1-8 Å wavelength band since 1994 (*Garcia*, 1994). As a measure of the average flare activity, the flux intensity, in units Wm^{-2}, is given as a letter (A, B, C, M, or X) together with a number. The letter represents a certain numeric value and the numbers following the letter in the classification multiply that value. The numeric values of the letter classes are given in Table 1. Daily readings of the X-ray background flux, available at NOAA Space Environment Center, are plotted in Figure 2, summarized in Table 4, and stored in the database as **noaa_dsd** (see Table 3).

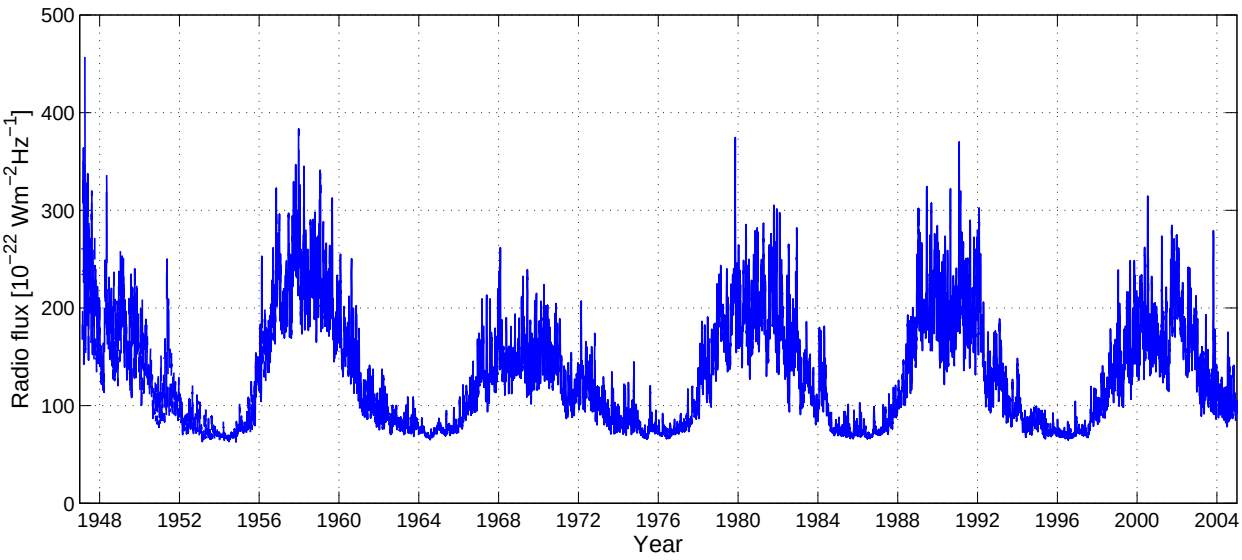

Figure 3: Daily values of observed solar radio flux at 2800 MHz (10.7 cm) in solar flux units from 1947 onwards.

Radio flux Radio flux, which originates from high in the Sun's chromosphere and lower corona, changes in response to sunspot activity. Radio intensity levels consist of emission from three sources: undisturbed solar surface, developing active regions, and short-lived enhancements above the daily level. Solar flux density at 2800 MHz, corresponding to a wavelength of 10.7 cm, has been recorded routinely by radio telescope since 1947 (*Covington*, 1969). This observational frequency/wavelength was set due to a historical coincidence and is now regarded as a typical wavelength for the entire radio spectrum.

Two sets of fluxes are available: observed and adjusted. The observed values are the least refined, since they contain fluctuations as large as 7% that arise from the changing Sun-Earth distance. In contrast, adjusted fluxes have this variation removed and the values equal the energy flux received by a detector located at a standard distance of 1 AU. The observed flux values are useful in solar-terrestrial studies like ionospheric physics. The adjusted fluxes are descriptive of the Sun's intrinsic behaviour.

The 10.7 cm solar flux correlates well with other indices of solar activity such as the sunspot number with the advantage that the measurements are more physics based, and can be made under almost any weather conditions. Observed radio flux at 2800 MHz, available at NOAA Space Environment Center, are plotted in Figure 3 and summarized in Table 4. Observed and adjusted radio fluxes are stored in the database as **noaa_radio** (see Table 3).

Solar wind parameters The solar wind and its interplanetary magnetic field (IMF) have been observed in situ since 1963, beginning with the Interplanetary Monitoring Platform No. 1 (IMP-1) (*Ness et al.*, 1964; *Paularena et al.*, 1997). Other important solar wind observing programmes are the WIND spacecraft (*Smith et al.*, 1998; *McComas et al.*, 1998), the three International Sun-Earth

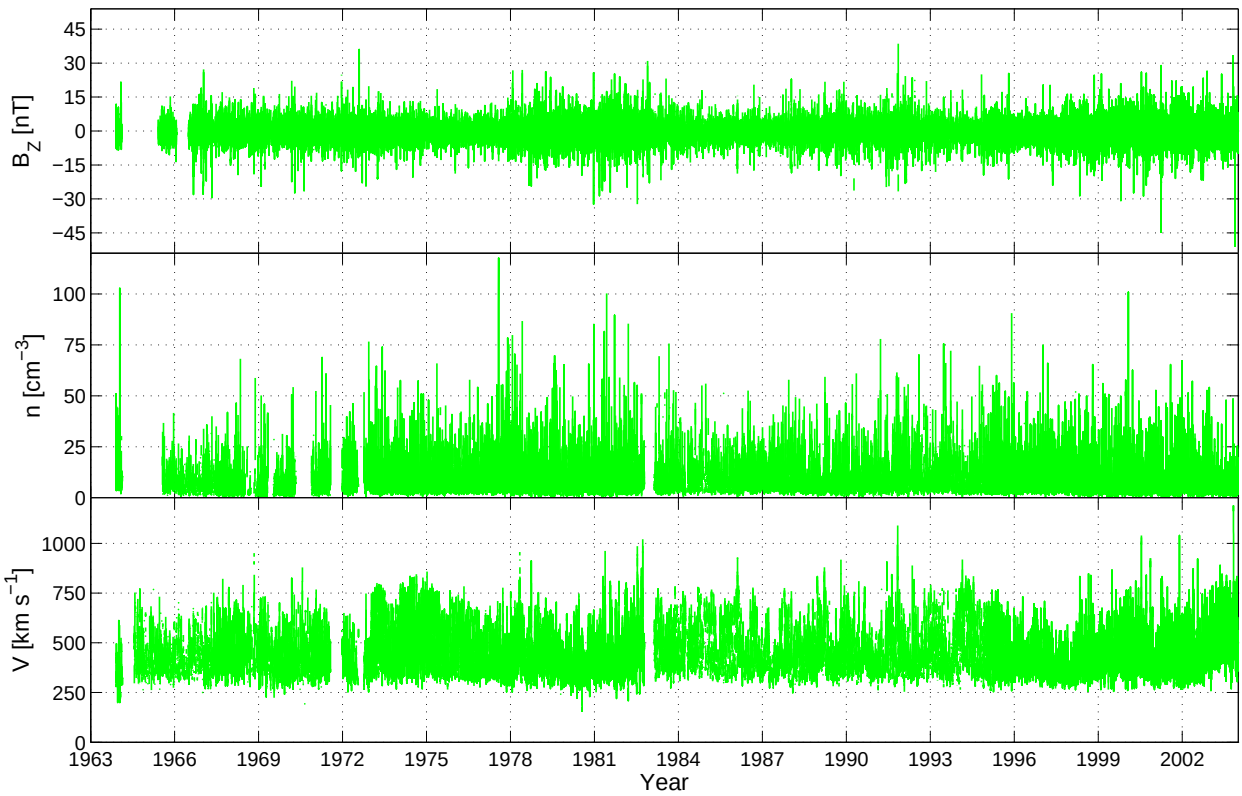

Figure 4: Composite plot of hourly averages of the interplanetary B_Z component in the GSM system, the solar wind proton density n, and the solar wind flow speed V for the period 1963-2003. Solar wind data are available in real-time but this plot gives the final processed values only.

Explorer (ISEE) spacecrafts (*Ogilvie et al.*, 1989), the Advanced Composition Explorer (ACE) (*Lepping et al.*, 1995; *Ogilvie et al.*, 1995), and the CELIAS/MTOF experiment onboard SOHO (*Ipavich et al.*, 1998).

The IMF is given in two coordinate systems, the Geocentric Solar Magnetospheric (GSM) system and the Geocentric Solar Ecliptic (GSE) system. The GSM system is a right-handed cartesian system centered on Earth with the x-axis directed towards the Sun and the z-axis located in the plane defined by the x-axis and the dipole axis. The GSE system has the z-axis perpendicular to the ecliptic plane. The GSM system is frequently used in solar-terrestrial studies and the most geoeffective component of the IMF is the B_Z component. Plasma parameters often used in solar-terrestrial studies are the flow speed V and the proton density n. The B_Z component together with the solar wind proton density and solar wind flow speed are plotted as hourly averages in Figure 4 and summarized in Table 4. Other solar wind parameters available from 1963 and onwards are the proton temperature, the flow pressure, and the electric field of the solar wind. A compilation of solar wind data, available at National Space Science Data Center, are stored in the database as **omni_2** (see Table 3).

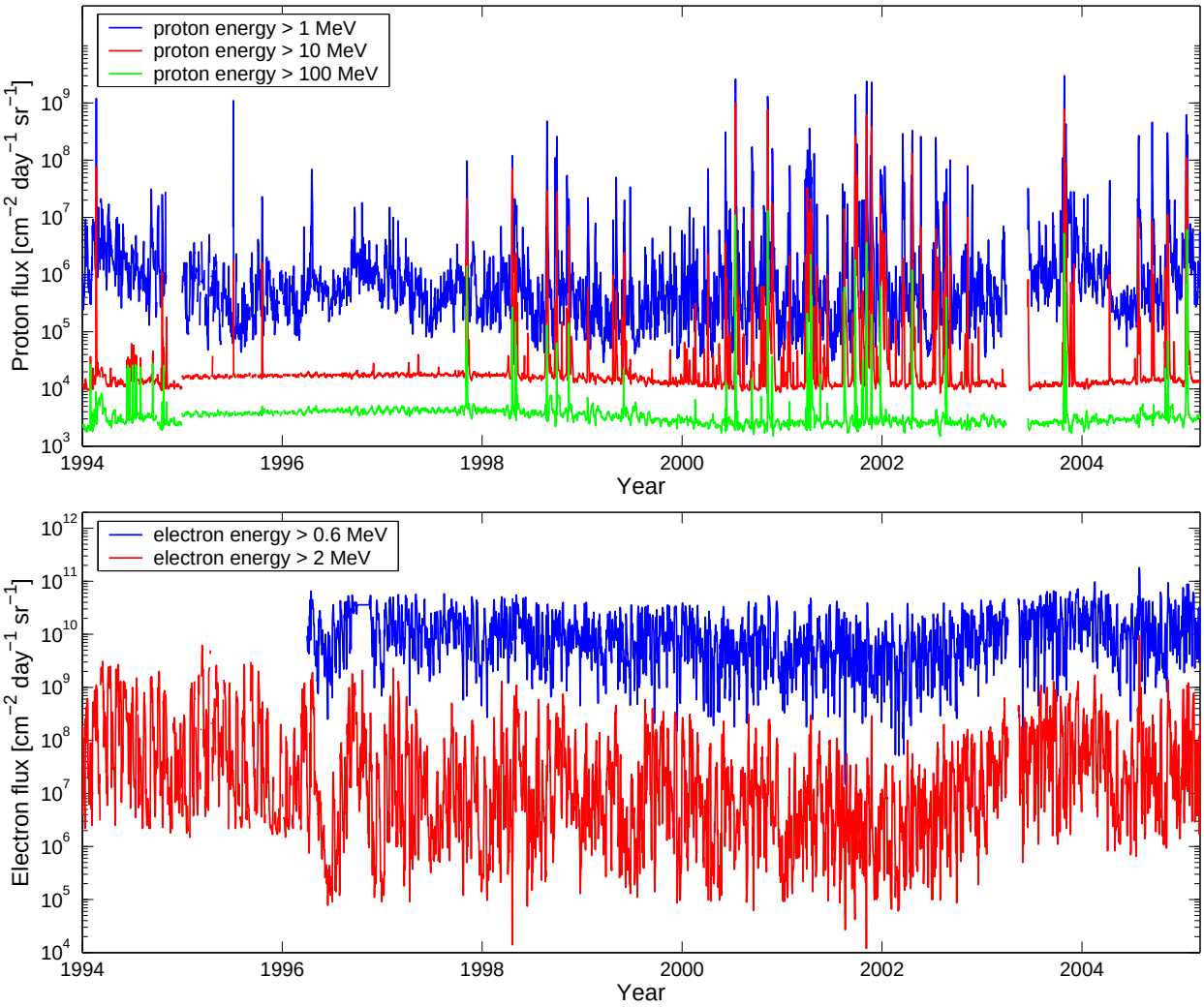

Figure 5: Daily sums of proton and electron fluxes from 1994. Note that colour coding is only to distinguish between different energy bands.

Proton and electron fluxes GOES spacecraft at geosynchronous orbits are used to measure levels of geomagnetically trapped and highly variable populations of protons and electrons (*Onsager et al.*, 1996). Integrated levels of proton fluxes are available for energies >1 MeV, >10 MeV, and >100 MeV in units protons cm^{-2} day^{-1} sr^{-1}. Integrated proton fluxes can be used to estimate the approximate amount of ionization occurring in the upper atmosphere as well as the proton penetration level into the atmosphere. Electron fluxes are given for energies >0.6 MeV and >2 MeV with the same units as the proton flux. Proton fluxes for three energy ranges and electron fluxes for two energy ranges, available at NOAA Space Environment Center, are plotted in Figure 5, summarized in Table 4, and stored in the database as **noaa_dpd** (see Table 3).

Magnetograms High resolution magnetograms have been recorded by the Michelson Doppler Imager (MDI) instrument onboard SOHO since 1995 (*Scherrer et al.*, 1995). These full-disc line-

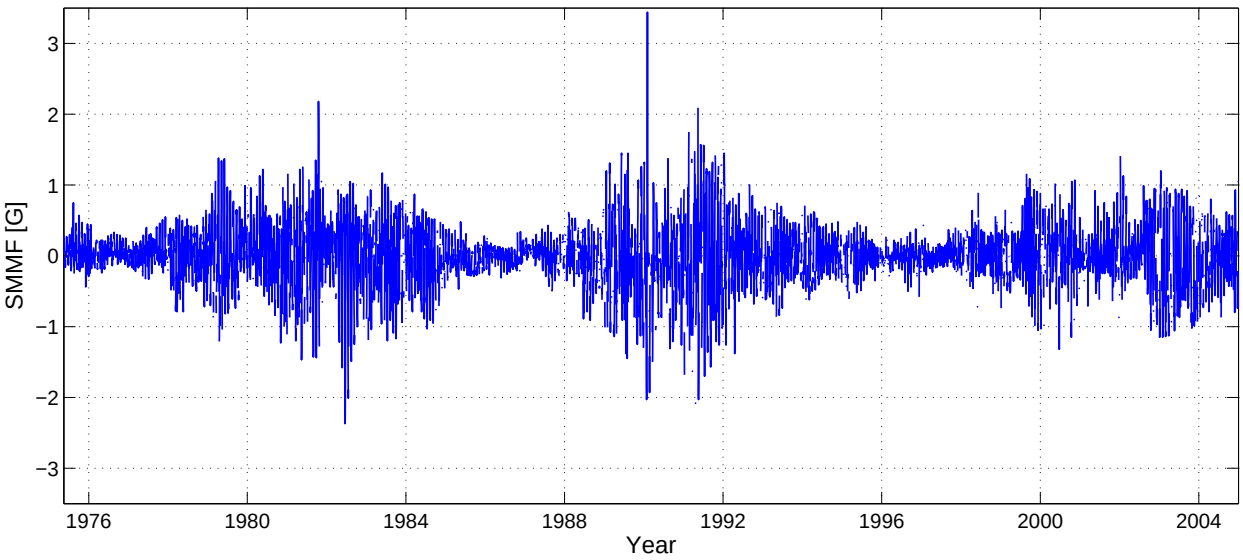

Figure 6: Plot of daily solar mean magnetic field measurements at Wilcox Solar Observatory from May 1975 to December 2004.

of-sight magnetograms are normally obtained every 96 minutes (15 per day), but during certain campaigns the resolution can be one magnetogram every minute. Using these magnetograms one can obtain solar information about the magnetic vector field, magnetic complexities, and stress gradients. The SOHO/MDI database is very extensive and due to limits in storage capacity not included in the ISAC database. The data is retrievable from the Solar Oscillations Investigation data archive at `http://soi.stanford.edu/data/data_request.html`.

Mean magnetic field The solar mean magnetic field (SMMF) is defined as the average field as observed over the entire visible disk (*García et al.*, 1999). As most field regions on the Sun have bipolar structures, the SMMF is relatively small with values rarely exceeding ±2 Gauss. SMMF measurements were first produced at the Crimean Astrophysical Observatory in 1968 (*Kotov and Severny*, 1983). These measurements continued until 1976. At the Mt. Wilson Observatory regular SMMF measurements were made between 1970 and 1982 (*Kotov et al.*, 1998). The Wilcox Solar Observatory (WSO) started their daily SMMF measurement programme in 1975 (*Scherrer et al.*, 1977) and it is still operational. SMMF values from WSO are plotted in Figure 6, summarized in Table 4, and stored in the database as **wso_smmf** (see Table 3).

Furthermore, SMMF measurements with a higher accuracy and a temporal resolution down to one minute can be extracted from magnetograms taken by the MDI instrument onboard SOHO from 1995 (*Scherrer et al.*, 1995; *Boberg et al.*, 2002). SMMF measurement have also been recorded by the GONG network consisting of six ground-based stations located around the Earth (*Harvey and the GONG Team*, 1998).

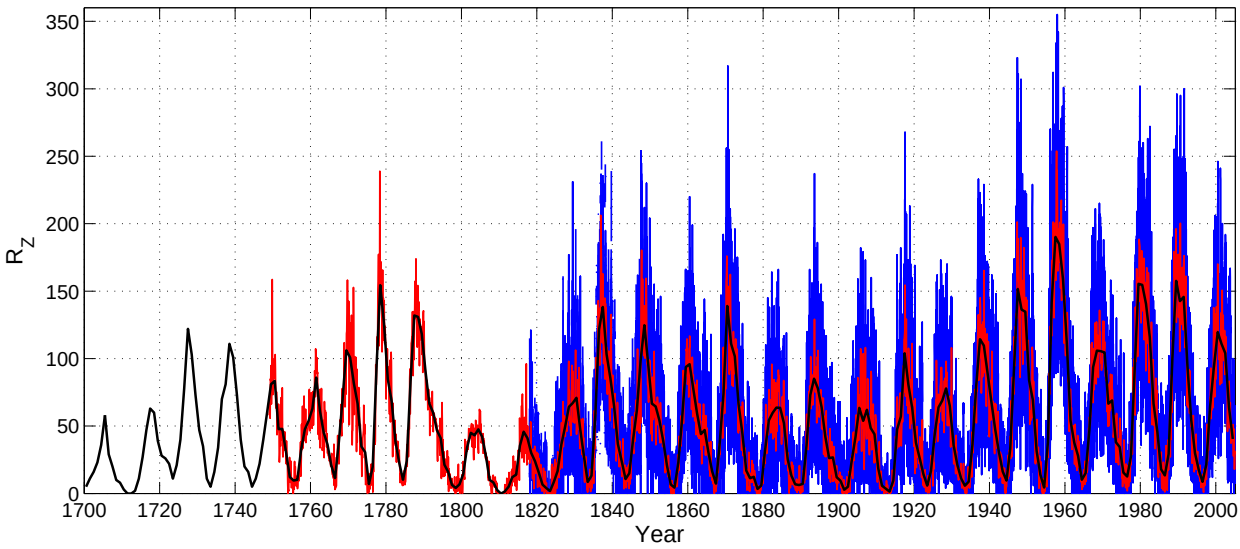

Figure 7: The relative sunspot number. Yearly averages (black) from 1700, monthly averages (red) from 1749, and daily readings (blue) from 1818 until present.

Harmonic coefficients of coronal magnetic field The magnetic field in the solar corona is difficult to measure in the visible spectrum with a useful spatial resolution. By using a potential field model (PFM), i.e. assuming that there are no electric currents, the coronal magnetic field can be computed in terms of spherical harmonic functions. The inner boundary condition to the model is the observed photospheric line-of-sight magnetic field. The outer boundary condition is a concentric surface placed at 2.5 solar radii at which the magnetic field is assumed to be radial. The computations are made once per solar rotation and the result is given as spherical harmonic coefficients (*Zhao and Hoeksema*, 1993). Harmonic coefficients of the coronal magnetic field, calculated using photospheric field maps since 1976 (Carrington rotation 1642) at Wilcox Solar Observatory, are stored in the database as **wso_gfhc** (see Table 3).

2.2 Indicators

The indicators presented in this section are classified as parameters that need to be interpreted before they can be used in solar-climate models. These indicators are divided into three categories: 1) indices (e.g. the sunspot number), 2) proxies (e.g. ^{14}C concentrations), and 3) lists (e.g. coronal mass ejection events).

2.2.1 Indices

Sunspot number The relative sunspot number was introduced in 1848 by Rudolf Wolf as a measure of activity of the entire visible disk of the Sun. It is determined each day without reference to preceding days. Each isolated cluster of sunspots is termed a sunspot group, and it may be composed of one or more than a hundred single distinct spots whose individual size can range from

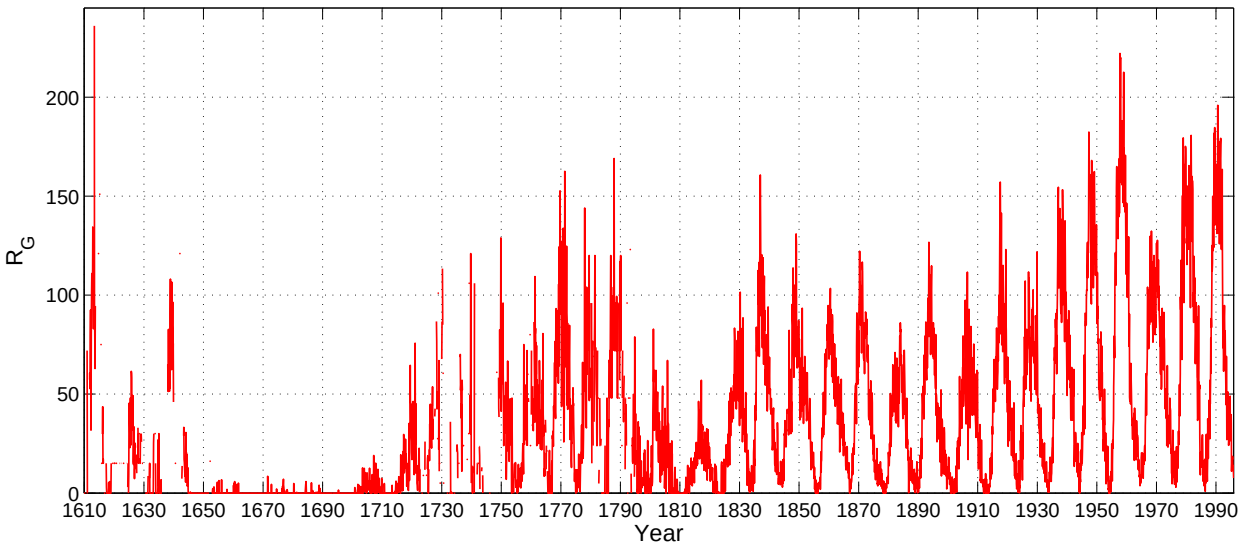

Figure 8: Monthly means of the group sunspot number for 1610-1995.

several square degrees down to the limit of resolution. The relative sunspot number, also know as the Wolf or Zürich Sunspot Number (*Waldmeier*, 1961), is defined as

$$R_Z = k(10g + n), \tag{1}$$

where g is the number of sunspot groups, n is the total number of individual spots, and k is the correction factor depending on the observer and is intended to effect the conversion to the scale originated by Wolf. The significance of the sunspot number lies first in the fact that they can be extracted far back in time. Daily readings available from 1818, monthly averages from 1749, and yearly averages from 1700, available at Solar Influences Data analysis Center, are given in Figure 7, summarized in Table 4, and stored in the database as **sidc_ssn** (see Table 3).

Group sunspot number The group sunspot number R_G was constructed to provide a homogeneous record of solar activity (*Hoyt and Schatten*, 1992, 1998). The group sunspot number is defined as

$$R_G = \frac{12.08}{N} \sum k_i' G_i, \tag{2}$$

where G_i is the number of sunspot groups recorded by the ith observer, k_i' is the ith observer's correction factor, N is the number of observers used to form the daily value, and 12.08 is a normalization factor chosen to make the mean R_G's identical with the mean R_Z's for the period 1874 to 1976. Compared with the sunspot number, R_G is more internally self-consistent and less noisy due to a large number of observations available and the exclusion of resolution limit errors for small individual sunspots. Monthly averages of R_G for the period 1610 to 1995, available at NOAA National Geophysical Data Center, are plotted in Figure 8 and summarized in Table 4. These monthly values together with the number of days used to form the means and the adherent standard deviation of the means are stored in the database as **noaa_gssn** (see Table 3).

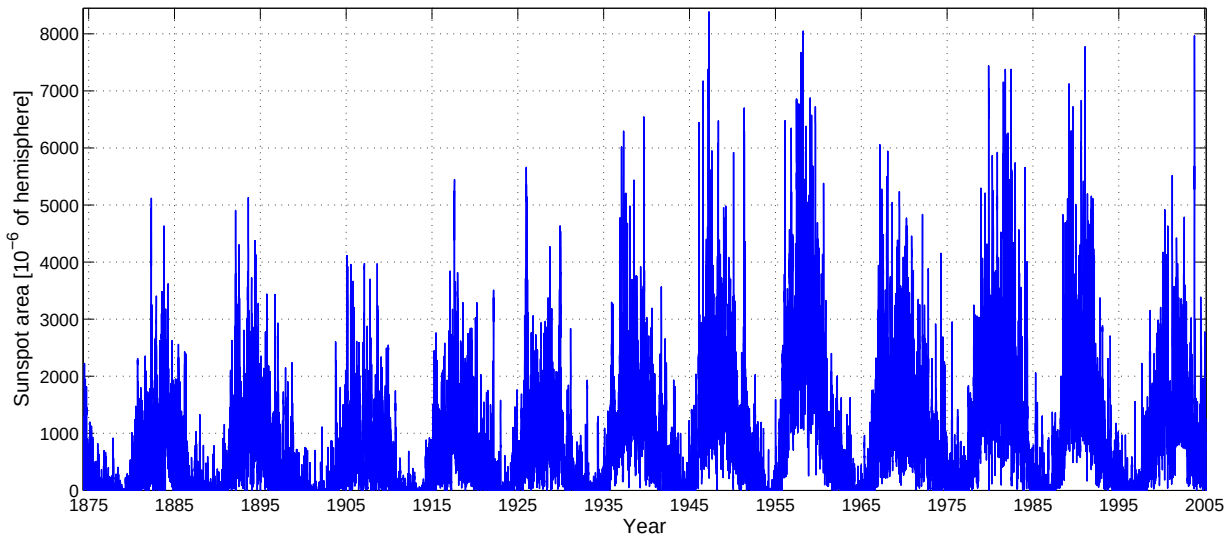

Figure 9: Daily values of the total sunspot area, in millionths of the visible solar hemisphere from 1874.

Sunspot area index Daily measurements of the total sunspot area begun at the Greenwich Heliophysical Observatory in 1874 and continued until 1976. Later measurements have been distributed by US Air Force and the Space Environment Center at NOAA. The total sunspot area is the sum of all visible sunspots, corrected for projection effects and given as 10^{-6} of the solar hemisphere (*Steinegger et al.*, 1996; *Győri*, 1998). Daily sunspot area numbers are plotted in Figure 9, summarized in Table 4, and stored in the database as **noaa_ssa** (see Table 3).

Magnetic plage strength index & Mt. Wilson sunspot index The magnetic plage strength index (MPSI) and Mt. Wilson sunspot index (MWSI) have been calculated at Mt. Wilson Observatory since 1970 (*Parker et al.*, 1997; *Ballester et al.*, 2004). The MPSI is determined from magnetograms by summing the absolute values of the magnetic field strengths for all pixels where the absolute value of the magnetic field strength is between 10 and 100 G. This number is then divided by the total number of pixels in the magnetogram. The MWSI values are subsequently determined by summing pixels with absolute values of the magnetic field strength greater than 100 G and then divided by the total number of pixels in the magnetogram. Daily MPSI and MWSI measurements are plotted in Figure 10, summarized in Table 4, and stored in the database as **mtwil_mag** (see Table 3).

Plage area index Plages are bright structures in the solar chromosphere particularly prominent in images obtained in the Ca II line at 393.4 nm. The total magnetic flux of plage regions is comparable to that of sunspots. Furthermore, radiation from magnetic plages has a large contribution to solar UV and EUV making plages a suitable measure of solar activity. A daily plage index has been derived from Ca II images of the Sun at Mt. Wilson during the period 1915-1984 (*Foukal*, 1996). The plage index is given as the total area of the calcium plages, given as a fraction of the visible solar hemisphere. Solar plage area data, available at NOAA National Geophysical Data Center,

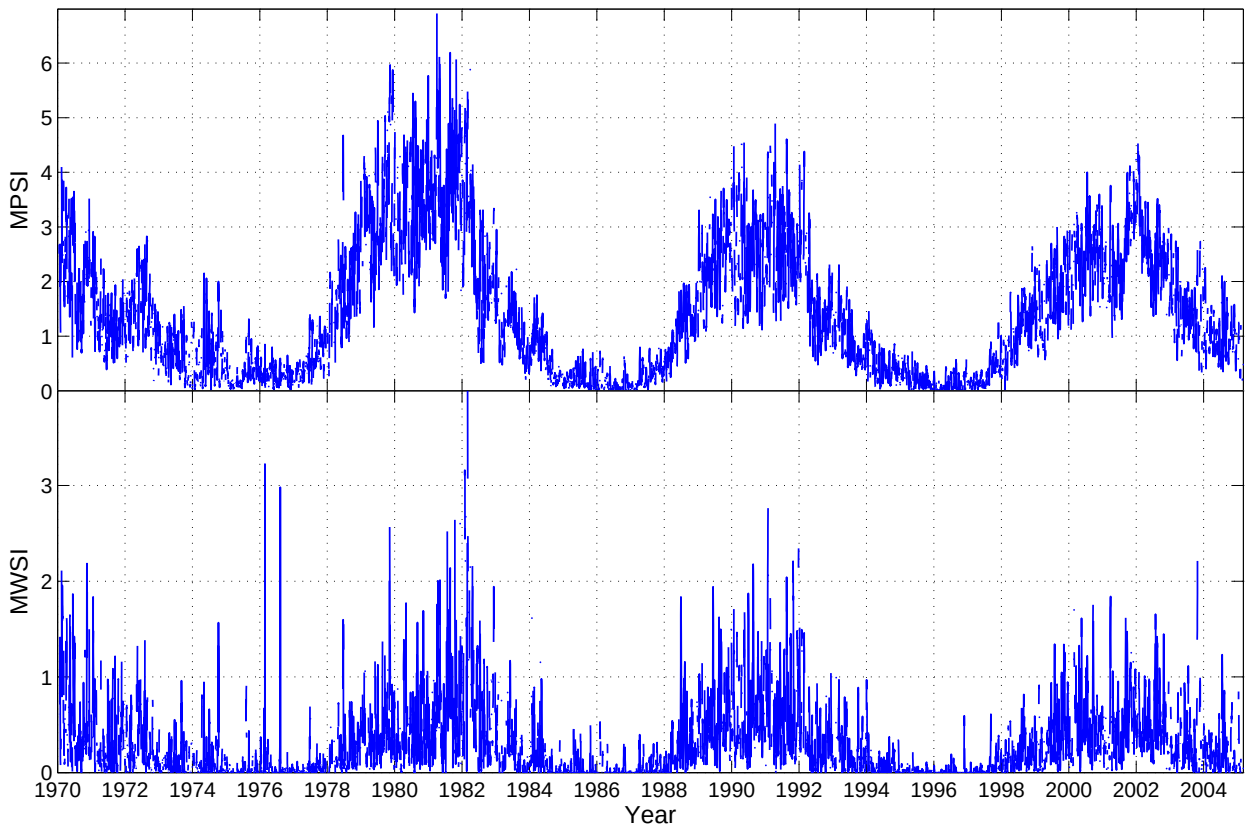

Figure 10: Daily calculations of the magnetic plage strength index and Mt. Wilson sunspot index from 1970 onwards.

are plotted in Figure 11, summarized in Table 4, and stored in the database as **noaa_plage** (see Table 3).

Solar UV index Solar ultraviolet (UV) radiation is located in the wavelength band between 120 and 400 nm and originates from the upper photosphere and the chromosphere. It comprises less than 1% of the total solar irradiance but has a strong direct impact on Earth's atmosphere and a considerable sunspot cycle variation of up to 10-20%. Early measurements of solar UV irradiance were made using rocket experiments (*Lean*, 1987). The observational confidence level and technique were steadily improved starting in the early 1980 using satellite observations such as the NOAA weather satellites (*Cebula et al.*, 1998) or the SOLSTICE spectrometer (*Woods et al.*, 1993; *Rottman*, 2000).

The level of solar UV radiation is often described using measurements of the Mg II absorption line at 280 nm (*DeLand and Cebula*, 1993). The resulting UV index is a dimensionless quantity measuring mid-UV solar activity. It is defined as the ratio of the irradiance in the core of the unresolved Mg II H & K doublet to the nearby continuum irradiance (*Cebula et al.*, 1992). Currently, the UV index data set contains daily values from 1978 onwards based on measurements from 6 different satellites (*Viereck and Puga*, 1999) and is available in real-time from NOAA Space Environment

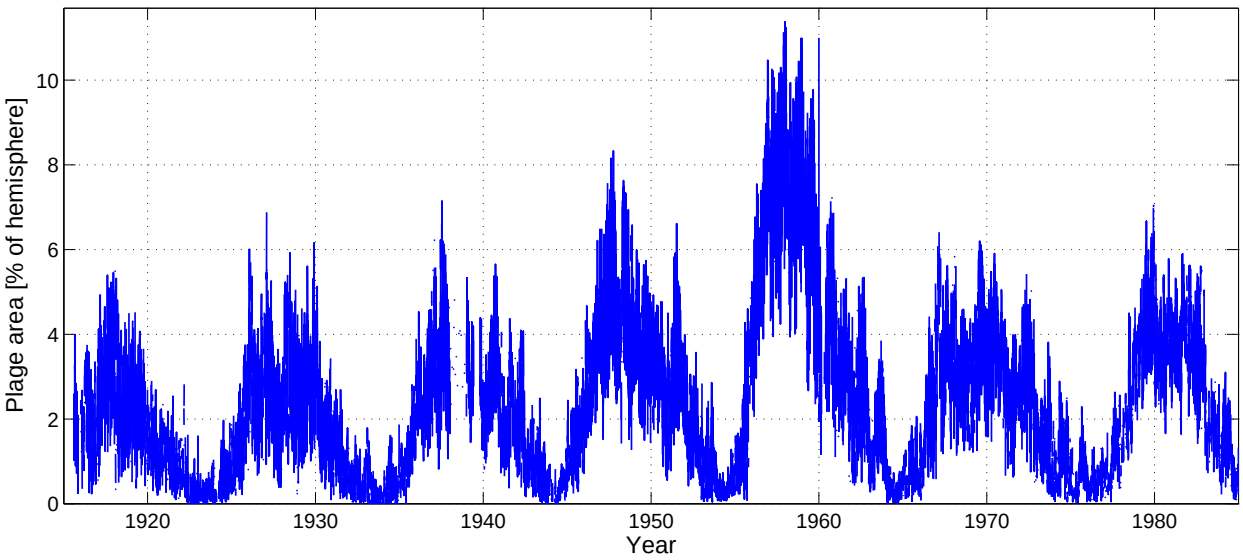

Figure 11: Daily measurements from 1915 to 1984 of the total plage area, in % of the visible solar hemisphere.

Center. The composite data are plotted in Figure 12, summarized in Table 4, and stored in the database as **noaa_uv** (see Table 3).

Solar EUV index Solar extreme ultraviolet (EUV) radiation is produced by magnetic activity in the solar chromosphere and corona. EUV radiation is not continuously measured but a proxy ($E_{10.7}$) has been developed based on radio flux measurements at 10.7 cm (*Tobiska*, 2001). $E_{10.7}$ offers significant improvement as an index of the energy input to the thermosphere and ionosphere. $E_{10.7}$ is similar to the radio flux at 10.7 cm when averaged over longer periods (months/years) but show distinct differences on a daily basis. The EUV proxy, available at NOAA National Geophysical Data Center, is plotted in Figure 13, summarized in Table 4, and stored in the database as **noaa_euv** (see Table 3).

Optical flare index The daily flare activity can be expressed as $F = I \times t$, where I is the intensity and t the duration in minutes of a solar flare event, giving an estimation of the total energy emitted by the flares (*Ataç and Özgüç*, 1998). The importance coefficient I of the flare is related to the optical flare classification according to Table 2. As a measure of relatively short-lived solar phenomena, the daily flare index F is available from 1976 onwards. The index is given for northern and southern hemispheres separately as well as a total value. To obtain final daily values, the daily sums of the index for the northern and southern hemispheres and for the total surface are divided by the total time of observation. Daily values, available at NOAA National Geophysical Data Center, from 1976 to 2002 are given in Figure 14, summarized in Table 4, and stored in the database as **noaa_flare** (see Table 3).

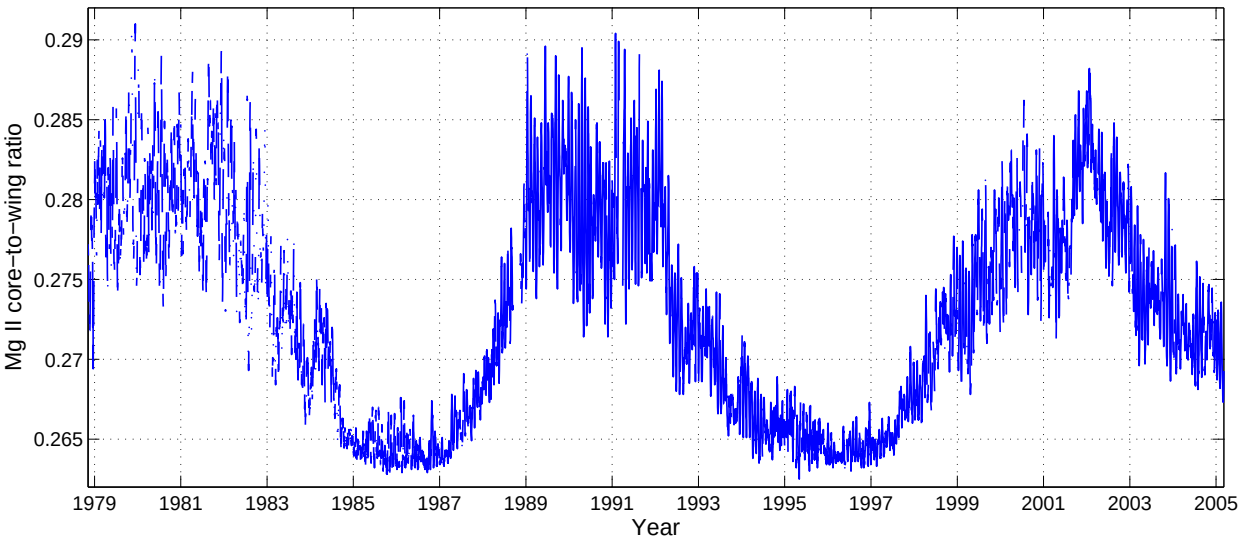

Figure 12: Top panel gives the Mg II core-to-wing ratio from 1978, as a measure of the solar UV output.

Importance	I	Importance	I
SF, SN, SB	0.5	2B	2.5
1F, 1N	1.0	3F, 3N, 4F	3.0
1B	1.5	3B, 4N	3.5
2F, 2N	2.0	4B	4.0

Table 2: Relationship between optical flare importance and importance coefficient I. The optical brightness and size of the flare are indicated by a two-character code called importance. The first character is a number from 1 to 4, indicating the apparent area. For areas of less than 1, an S is used to designate a subflare. The second character indicates relative brilliance: B for bright, N for normal, and F for faint.

Coronal index The coronal index (*CI*) (*Rybanský et al.*, 1994b,a) measures the total energy emitted by the solar corona at a wavelength of 530.3 nm into one sterradian towards the Earth. *CI* is available with daily values for the period 1939 to 2002, based on observations made at up to 8 ground based stations. All line emissions have been converted with a linear transformation to a common intensity scale by shifting position angles of the measurements and by comparing values taken at all the sites. 64 years of *CI* measurements, available at NOAA National Geophysical Data Center, are plotted in Figure 15, summarized in Table 4, and stored in the database as **noaa_coronal** (see Table 3).

2.2.2 Geomagnetic indices

Although geomagnetic indices do not represent solar output data they have been included for magnetosphere–ionosphere interaction studies.

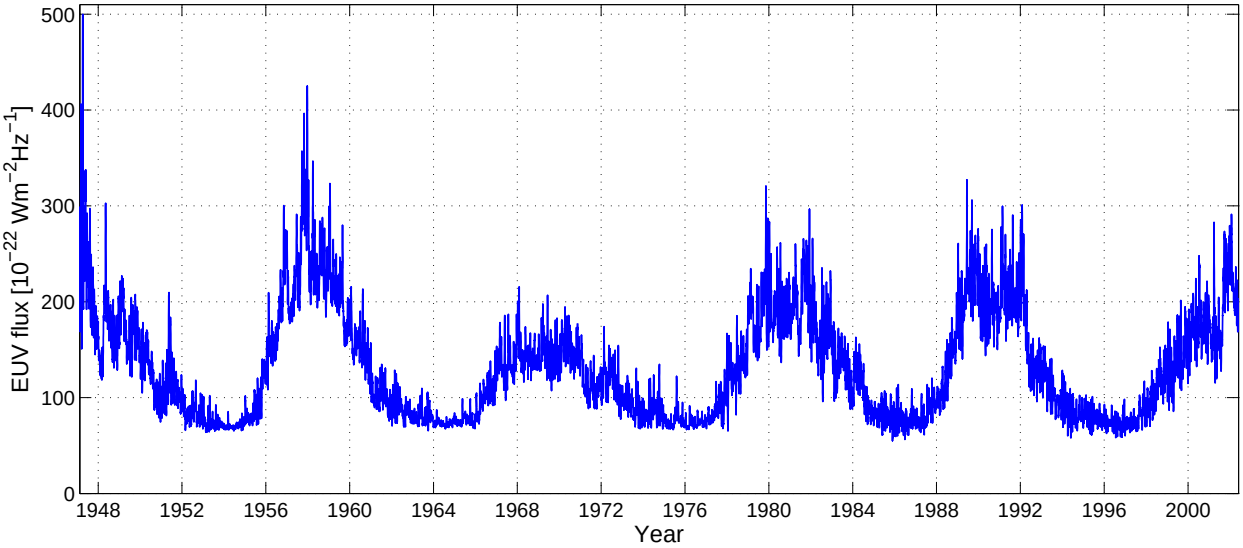

Figure 13: Daily EUV calculations from 1947 onwards.

Dst The *Dst* index was created to study the ring current in the equatorial plane at 3 4 R_E (*Sugiura*, 1964; *Mayaud*, 1980). *Dst* is deviation of the horizontal magnetic field component measured at four near-equatorial stations evenly distributed in longitude. The temporal resolution is one hour and covers the period 1957–April 2005 (Figure 16). The data from 2004 and onwards contain both estimated and preliminary values, while the data before that are final.

Kp The *Kp* index is a planetary index indicating the level of geomagnetic activity (*Bartels*, 1949; *Mayaud*, 1980). Based on data from mid-latitude magnetic observatories on the northern hemisphere, the maximum deviation of the horizontal magnetic field in 3-hour intervals is computed. Finally, a quasi-logarithmic scaling is made into 28 symbols indicating different levels of activity so that $Kp \in \{0_0, 0_+, 1_-, 1_0, 1_+, \ldots, 8_-, 8_0, 8_+, 9_-, 9_0\}$. The *Kp* symbols are translated into integer values and stored in the database as $\{0, 3, 7, 10, 13, \ldots, 77, 80, 83, 87, 90\}$. The index is available from the International Service of Geomagnetic Indices (ISGI) and covers the period 1932–May 2005 (Figure 17). A summary is given in Table 4 and the data are stored in the database as **isgi_kp_ap** (see Table 3).

ap The *ap* index (*Mayaud*, 1980) is basically the *Kp* index but on a linear scale with units of nT. $Kp = 0_0$ corresponds to $ap = 0$ nT and $Kp = 9_0$ to $ap = 400$ nT. The index is also available from the International Service of Geomagnetic Indices (ISGI) and covers the period 1932–May 2005 (Figure 18). A summary is given in Table 4 and the data are stored in the database as **isgi_kp_ap** (see Table 3).

aa The *aa* index is based on measurements from two sub-auroral antipodal stations (Greenwich and Melbourne) (*Mayaud*, 1980), and the choice of only two stations were made so that the time

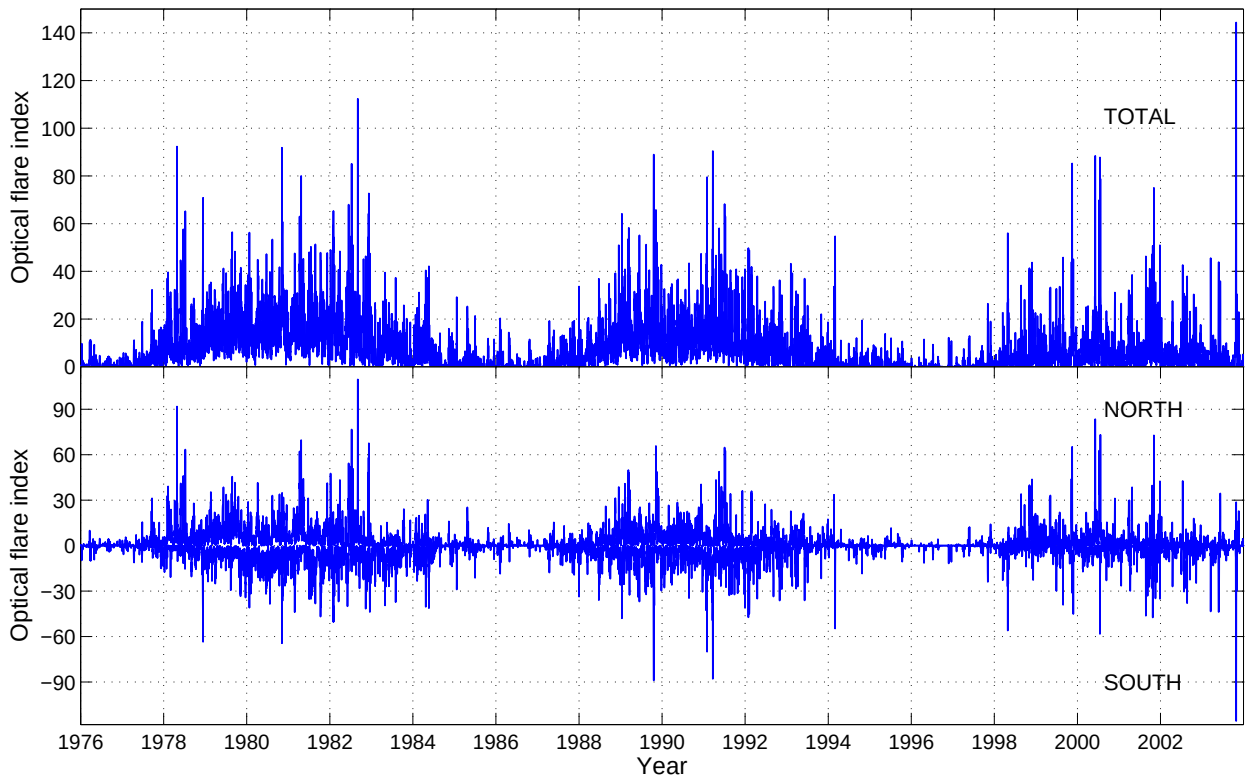

Figure 14: Daily observations of the flare activity F for the period 1976-2002. Top panel gives values for the full visible surface while the bottom panel give values for the two hemispheres separately.

series could be extended back in time as far as possible. Although the *aa* index is given with 3-hour resolution it is preferable to use daily values because with only two stations global disturbances are not described correctly on 3-hour intervals. The index is available from NOAA National Geophysical Data Center and covers the period 1868–May 2005 (Figure 19). A summary is given in Table 4 and the data are stored in the database as **noaa_aa** (see Table 3).

2.2.3 Proxies

Solar variability can be traced several hundred thousand years back in time using cosmogenic isotopes like ^{14}C and ^{10}Be (*Muscheler et al.*, 2003). These isotopes are radioactive and are produced by the interaction of galactic cosmic rays with atmospheric atoms, where the galactic cosmic ray infall is modulated by the solar wind. ^{10}Be, with a half-life of 1.5 million years, is more suitable to reconstruct solar activity over very long time periods, compared to ^{14}C with a half-live of 5,730 years. Furthermore, ^{14}C can provide global signals but is less reliable due to influences from natural carbon cycles. ^{14}C is produced mainly by the interaction of thermal neutrons with atmospheric nitrogen and shows up in tree ring measurements (*Stuiver et al.*, 1998). ^{10}Be interacts with aerosols and is subsequently removed from the atmosphere by wet deposition, making it measurable in natural archives such as ice cores (*Beer et al.*, 1990).

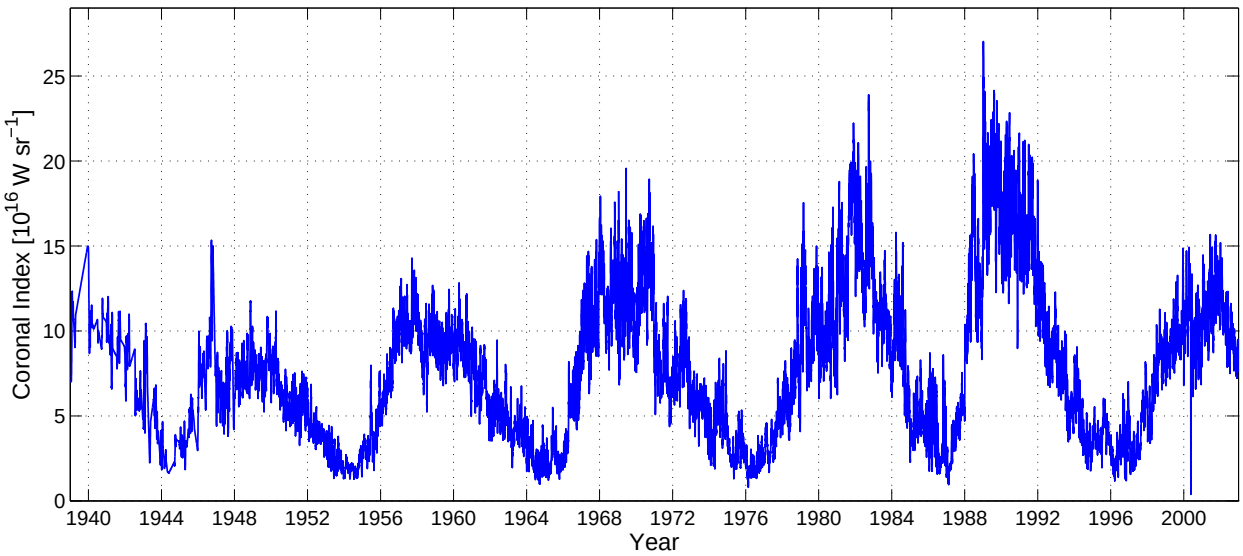

Figure 15: Daily readings of *CI*.

Bard et al. (2000) used fluctuations of ^{14}C and ^{10}Be production rates from an ice core at the South Pole to reconstruct solar irradiance from 843 to 1961 A.D. The productions rates and the solar irradiance reconstructions are available from NOAA National Climatic Data Center and included in the database as **noaa_iso_bard** (see Tables 3 and 4).

Finkel and Nishiizumi (1997) presented a record of ^{10}Be concentrations from the Greenland Ice Sheet Project 2 (GISP2) obtained from ice cores covering the period 3 to 40 kyr B.P. (1950 A.D.) These data are available from NOAA National Climatic Data Center and included in the ISAC database as **noaa_iso_gisp2** (see Tables 3 and 4).

The North Greenland Ice Core Project (NGRIP), using ice cores from central Greenland, have produced a climatic record of the oxygen isotopic composition ($\delta\,^{18}$O) (*North Greenland Ice Core Project members*, 2004). The data record, covering the period 0 to 123 kyr B.P. (2000 A.D.), is available from NOAA National Climatic Data Center and included in the ISAC database as **noaa_iso_ngrip** (see Tables 3 and 4).

2.2.4 Lists

Coronal mass ejections Coronal mass ejections (CMEs) are huge plasma clouds embedded in magnetic field structures that are ejected from the Sun (*Gosling*, 1997). CMEs become part of the solar wind as they propagate outwards, becoming Interplanetary CMEs (ICME). ICMEs disrupt the flow of the solar wind and produce significant disturbances that can interact with the Earth's environment (*Luhmann*, 1997). CMEs have been recorded since 1996 by the Large Angle Spectroscopic Coronagraph (LASCO) instrument onboard SOHO (*St. Cyr et al.*, 2000). These observations have been cataloged with such information as position angle, angular width, speed, and acceleration for each individual observed CME. This catalog, available by the Center for Solar

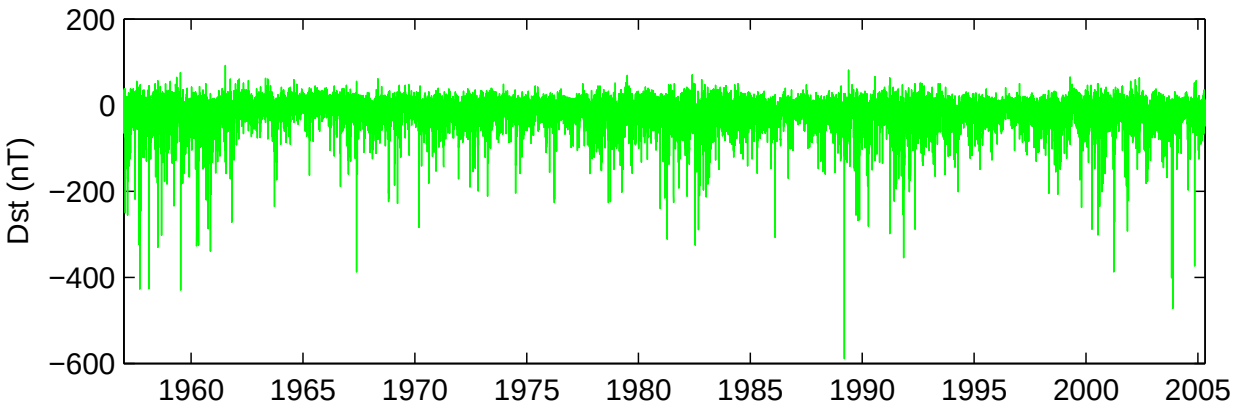

Figure 16: Hourly *Dst*.

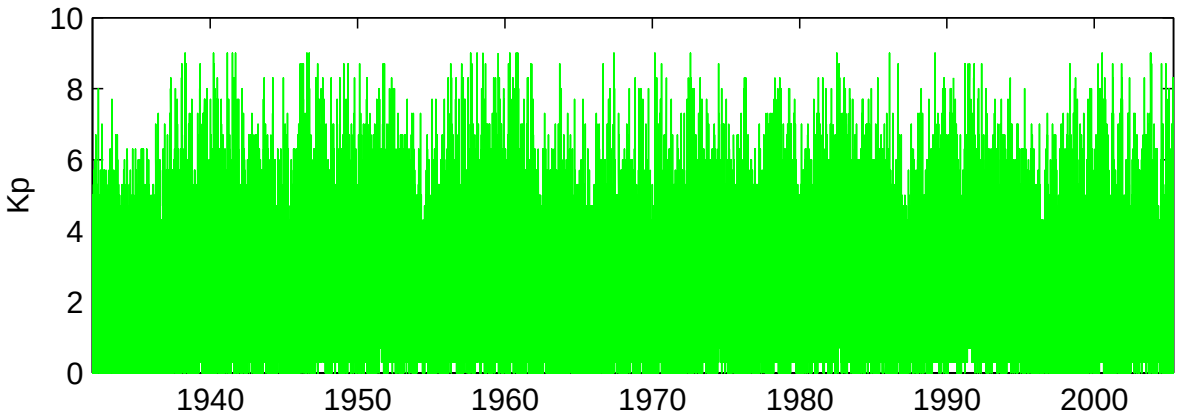

Figure 17: 3-hour *Kp*.

Physics and Space Weather, is included in our database as **sdac_cme** (see Tables 3 and 4).

X-ray flare events A solar flare is a sudden and rapid explosion on the Sun were energy stored in twisted magnetic fields is released. Flares produce a burst of radiation across the electromagnetic spectrum, from radio waves to X-rays and gamma-rays. Solar flares are classified according to their X-ray brightness in the wavelength range 1 to 8 Å. X-ray flare events from 1975 have been cataloged using measurements made by the GOES satellites (*Garcia*, 1994). An X-ray flare event list, with time interval, time of maximum intensity, total flux intensity, and origin on the solar disc for all individual events, is available at NOAA National Geophysical Data Center, summarized in Table 4, and stored in the database as **noaa_xraylist** (see Table 3).

Proton events Proton fluxes are given as 5-minute averages for energies >10 MeV, given in particles cm^{-2} sr^{-1} s^{-1} (pfu) measured by GOES spacecraft at geosynchronous orbit. Large proton fluxes are caused by high-energy solar flares and interplanetary shocks caused by ICMEs. The start

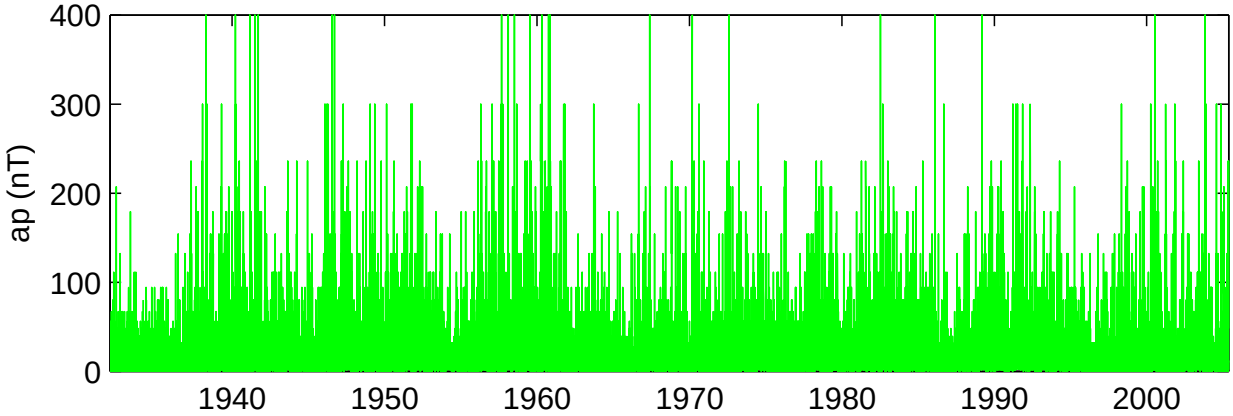

Figure 18: 3-hour *ap*.

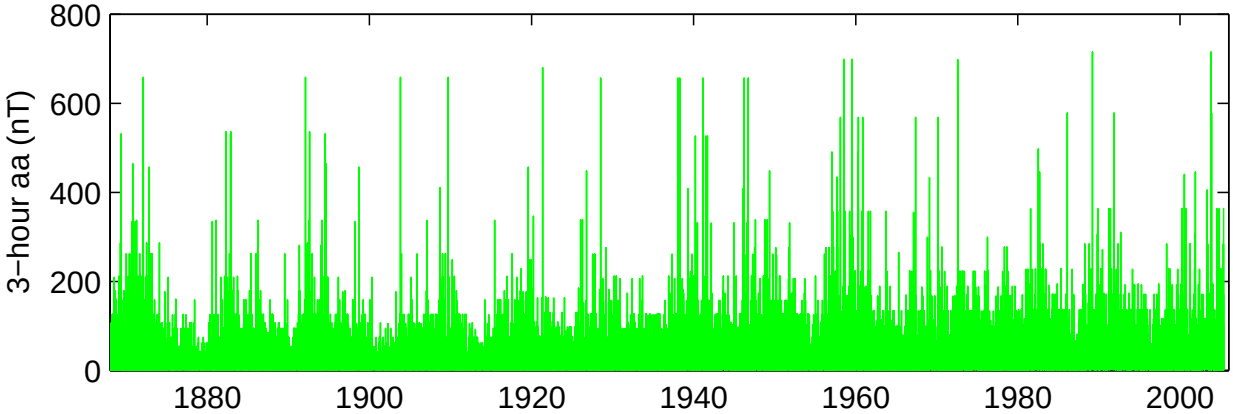

Figure 19: 3-hour aa.

of a proton event is defined as the first of three consecutive data points with fluxes greater than or equal to 10 pfu. The end of an event is the last time the flux was greater than or equal to 10 pfu. This definition allows multiple proton flares and/or interplanetary shock proton increases to occur within one proton event. A proton event list, with start and peak time and total proton flux for each event together with associated CME, flare, and active region, is available at NOAA National Geophysical Data Center, summarized in Table 4, and stored in the database as **noaa_pevent** (see Table 3).

3 Database

The solar data for this study are retrieved from a number of different databases. A short description of these databases are given below. This is followed by a presentation of our database named ISAC, including how to access the data and what information that comes with each data component.

3.1 Data sources

The sunspot number is retrieved from the Solar Influences Data analysis Center (SIDC) in Belgium. SIDC has been the World Data Center for the sunspot index since 1981 and serves as one out of 11 Regional Warning Centers (RWC) of the International Space Environment Service (ISES).

The National Geophysical Data Center (NGDC), located in Boulder, Colorado, is one of three NOAA National Data Centers. One aim of NGDC is to provide services for geophysical data describing the solar-terrestrial environment. NGDC currently maintain more than 300 digital and analog databases.

NOAA Space Environment Center (SEC) is one of nine National Centers for Environmental Prediction and provides real-time monitoring and forecasting of solar and geophysical events, conducts research in solar-terrestrial physics, and develops techniques for forecasting solar and geophysical disturbances.

The Wilcox Solar Observatory (WSO), located near Stanford University, California, began daily observations of the Sun's global magnetic field in 1975, with the goal of understanding changes in the Sun and how those changes affect the Earth. WSO produces low-resolution photospheric field maps used to produce daily solar mean field values as well as calculate the coronal magnetic field.

A coronal mass ejection (CME) catalog based on SOHO/LASCO observations is maintained by the Solar Data Analysis Center (SDAC) at NASA Goddard Space Flight Center in Greenbelt, Maryland. The catalog is developed using the SOHO data in cooperation with the Naval Research Laboratory and currently contains almost 9000 CME events.

Mt. Wilson Observatory, located in the San Gabriel Mountains in Southern California, have made solar observations for more than 100 years. Photospheric magnetograms taken by the 150-foot Solar Tower from 1970 have been used to derive two indices (magnetic plage strength index and Mt. Wilson sunspot index) described in this report.

3.2 ISAC database

The solar data presented in this report are stored in a MySQL (*DuBois*, 2003) database at the Swedish Institute of Space Physics. The database is named `isac` and contains solar data organised in tables according to the data sources described in Table 3. In total there are 19 tables in the database and each table is described in the Appendix and summarized in Table 3.

Name	Parameter(s)	Data Source
isgi_aa	*aa* index	International Service of Geomagnetic Indices
http://www.cetp.ipsl.fr/∼isgi/source/indices/aa/aa.doc http://www.cetp.ipsl.fr/∼isgi/source/indices/aa/aa1868.ima ⋮ http://www.cetp.ipsl.fr/∼isgi/source/indices/aa/aa2005.ima		
isgi_kp_ap	*Kp* & *ap* indices	International Service of Geomagnetic Indices
http://www.cetp.ipsl.fr/∼isgi/source/indices/Kp/kp-ap.doc http://www.cetp.ipsl.fr/∼isgi/source/indices/Kp/kp1932.wdc ⋮ http://www.cetp.ipsl.fr/∼isgi/source/indices/Kp/kp2005.wdc		
mtwil_mag	Plage & sunspot index	Mt. Wilson Observatory
ftp://howard.astro.ucla.edu/pub/obs/mpsi_data/index.dat		
noaa_coronal	Coronal index	NOAA National Geophysical Data Center
ftp://ftp.ngdc.noaa.gov/STP/SOLAR_DATA/SOLAR_CORONA/INDEX/daily_revised.plt ftp://ftp.ngdc.noaa.gov/STP/SOLAR_DATA/SOLAR_CORONA/INDEX/1999 ⋮ ftp://ftp.ngdc.noaa.gov/STP/SOLAR_DATA/SOLAR_CORONA/INDEX/2002		
noaa_dpd	Proton/electron flux	NOAA Space Environment Center
http://www.sec.noaa.gov/ftpdir/indices/old_indices/1994_DPD.txt ⋮ http://www.sec.noaa.gov/ftpdir/indices/old_indices/2004_DPD.txt http://www.sec.noaa.gov/ftpdir/indices/old_indices/2005Q1_DPD.txt http://www.sec.noaa.gov/ftpdir/indices/old_indices/2005Q2_DPD.txt		
noaa_dsd	X-ray flux	NOAA Space Environment Center
http://www.sec.noaa.gov/ftpdir/indices/old_indices/1994_DSD.txt ⋮ http://www.sec.noaa.gov/ftpdir/indices/old_indices/2004_DSD.txt http://www.sec.noaa.gov/ftpdir/indices/old_indices/2005Q1_DSD.txt http://www.sec.noaa.gov/ftpdir/indices/old_indices/2005Q2_DSD.txt		
noaa_dst	*Dst* index	NOAA National Geophysical Data Center
ftp://ftp.ngdc.noaa.gov/STP/GEOMAGNETIC_DATA/INDICES/DST/dst.fmt ftp://ftp.ngdc.noaa.gov/STP/GEOMAGNETIC_DATA/INDICES/DST/dst1957 ⋮ ftp://ftp.ngdc.noaa.gov/STP/GEOMAGNETIC_DATA/INDICES/DST/dst2001 ftp://ftp.ngdc.noaa.gov/STP/GEOMAGNETIC_DATA/INDICES/DST/dst2002.final ftp://ftp.ngdc.noaa.gov/STP/GEOMAGNETIC_DATA/INDICES/DST/dst2003 ftp://ftp.ngdc.noaa.gov/STP/GEOMAGNETIC_DATA/INDICES/DST/dst2004 ftp://ftp.ngdc.noaa.gov/STP/GEOMAGNETIC_DATA/INDICES/DST/dst2005.v4		
noaa_euv	Extreme UV index	NOAA National Geophysical Data Center
ftp://ftp.ngdc.noaa.gov/STP/SOLAR_DATA/SOLAR_UV/SOLAR2000/Five_cycle_v1_23a.txt		
noaa_flare	Flare index	NOAA National Geophysical Data Center
ftp://ftp.ngdc.noaa.gov/STP/SOLAR_DATA/SOLAR_FLARES/INDEX/daily21.plt ⋮ ftp://ftp.ngdc.noaa.gov/STP/SOLAR_DATA/SOLAR_FLARES/INDEX/daily23.plt		
noaa_gssn	Group sunspot number	NOAA National Geophysical Data Center
ftp://ftp.ngdc.noaa.gov/STP/SOLAR_DATA/SUNSPOT_NUMBERS/GROUP_SUNSPOT_NUMBERS/monthrg.dat		

Table 3 continued on next page...

Table 3 – continued

Name	Parameter(s)	Data Source
noaa_iso_bard	^{14}C, ^{10}Be production rates	NOAA National Climatic Data Center
ftp://ftp.ncdc.noaa.gov/pub/data/paleo/climate_forcing/solar_variability/bard_irradiance.txt		
noaa_iso_gisp2	^{10}Be concentration	NOAA National Climatic Data Center
ftp://ftp.ncdc.noaa.gov/pub/data/paleo/icecore/greenland/summit/gisp2/cosmoiso/ber10.txt		
noaa_iso_ngrip	$\delta\,^{18}$O composition	NOAA National Climatic Data Center
ftp://ftp.ncdc.noaa.gov/pub/data/paleo/icecore/greenland/summit/ngrip/isotopes/ngrip-d18o-50yr.txt		
noaa_pevents	Proton event list	NOAA National Geophysical Data Center
ftp://ftp.ngdc.noaa.gov/STP/SOLAR_DATA/Satellite_ENVIRONMENT/PARTICLES/p_events.lst		
noaa_plage	Plage area index	NOAA National Geophysical Data Center
ftp://ftp.ngdc.noaa.gov/STP/SOLAR_DATA/SOLAR_CALCIUM/DATA/MTWILSON/mtwl1915.cal ⋮ ftp://ftp.ngdc.noaa.gov/STP/SOLAR_DATA/SOLAR_CALCIUM/DATA/MTWILSON/mtwl1984.cal		
noaa_radio	Radio flux	NOAA Space Environment Center
ftp://ftp.ngdc.noaa.gov/STP/SOLAR_DATA/SOLAR_RADIO/FLUX/DAILYPLT.OBS ftp://ftp.ngdc.noaa.gov/STP/SOLAR_DATA/SOLAR_RADIO/FLUX/DAILYPLT.ADJ		
noaa_ssa	Sunspot area	NASA Science Directorate
http://science.nasa.gov/ssl/pad/solar/greenwch/daily_area.txt		
noaa_tsi_comp	Total solar irradiance	NOAA National Geophysical Data Center
ftp://ftp.ngdc.noaa.gov/STP/SOLAR_DATA/SOLAR_IRRADIANCE/composite_d25_07_0310a.dat		
noaa_uv	UV index	NOAA Space Environment Center
http://www.sec.noaa.gov/ftpdir/sbuv/NOAAMgII.dat		
noaa_xraylist	X-ray flare list	NOAA National Geophysical Data Center
ftp://ftp.ngdc.noaa.gov/STP/SOLAR_DATA/SOLAR_FLARES/XRAY_FLARES/xray1975 ⋮ ftp://ftp.ngdc.noaa.gov/STP/SOLAR_DATA/SOLAR_FLARES/XRAY_FLARES/xray1977 ftp://ftp.ngdc.noaa.gov/STP/SOLAR_DATA/SOLAR_FLARES/XRAY_FLARES/xray1978.corrected ftp://ftp.ngdc.noaa.gov/STP/SOLAR_DATA/SOLAR_FLARES/XRAY_FLARES/xray1979 ⋮ ftp://ftp.ngdc.noaa.gov/STP/SOLAR_DATA/SOLAR_FLARES/XRAY_FLARES/xray2003 ftp://ftp.ngdc.noaa.gov/STP/SOLAR_DATA/SOLAR_FLARES/XRAY_FLARES/xray2004.REVISED ftp://ftp.ngdc.noaa.gov/STP/SOLAR_DATA/SOLAR_FLARES/XRAY_FLARES/xray2005.2		
omni_2	Solar wind parameters	National Space Science Data Center
ftp://nssdcftp.gsfc.nasa.gov/spacecraft_data/omni/omni2_1963.dat ⋮ ftp://nssdcftp.gsfc.nasa.gov/spacecraft_data/omni/omni2_2003.dat		
sdac_cme	Coronal mass ejection list	Center for Solar Physics and Space Weather
http://cdaw.gsfc.nasa.gov/CME_list/UNIVERSAL/text_ver/univ_all.txt		
sidc_ssn	Sunspot number	Solar Influences Data analysis Center
http://sidc.oma.be/DATA/dayssn_import.dat http://sidc.oma.be/DATA/monthssn.dat http://sidc.oma.be/DATA/yearssn.dat		
wso_gfhc	Coronal harmonic coefficients	Wilcox Solar Observatory
http://soi.stanford.edu/∼wso/Harmonic.los/CR1642		

Table 3 continued on next page...

Table 3 – continued

Name	Parameter(s)	Data Source
⋮		
http://soi.stanford.edu/∼wso/Harmonic.los/CR2026		
wso_smmf	Mean magnetic field	Wilcox Solar Observatory
http://soi.stanford.edu/∼wso/meanfld/timeseries		
http://soi.stanford.edu/∼wso/meanfld/mf.2001.modif		
http://soi.stanford.edu/∼wso/meanfld/mf.2002.modif		
http://soi.stanford.edu/∼wso/meanfld/mf.2003		
http://soi.stanford.edu/∼wso/meanfld/mf.2004		
http://soi.stanford.edu/∼wso/meanfld/mf.2005		

Table 3: A summary of solar activity data with references to database and data source including a web address.

Each database table consists of at least 2 columns, where the first column contains the time stamps of the observations and the following columns contain the data. The time stamp is a `DATE` type if the temporal resolution is days or longer, else `DATETIME` type is used. To each table there is also associated meta-data that contain a short description of the data. The data are retrieved from the database using SQL queries. The output from the query may be in many different formats, e.g. as ASCII tables or in Matlab© format. Below we show how to retrieve data in different environments.

3.2.1 Command prompt

Firstly, one needs to connect to the database. This is done with the mysql command using the following flags:

```
mysql isac -h rwc.lund.irf.se -u isac -p
```

where `isac` selects the isac database, `-h` indicates the host, `-u` the user, and `-p` that a password needs to be specified. In this case the password is `maunder`. At this stage the command prompt

```
isac@rwc.lund.irf.se>
```

should appear. If this does not work then the `mysql` program must be installed. It can be found at the MySQL[1] web page. The tables can be listed with the command

```
show tables;
```

[1] http://www.mysql.com

```
+----------------+
| Tables_in_isac |
+----------------+
| mtwil_mag      |
| noaa_coronal   |
   ...
| wso_gfhc       |
| wso_smmf       |
+----------------+
24 rows in set (0.06 sec)
```

To extract all MtWilson data, ordered in time, the following SQL query may be used:

```
select * from mtwil_mag order by dt;
+------------+-----------+-----------+
| dt         | mpsi      | mwsi      |
+------------+-----------+-----------+
| 1970-01-19 |  2.5104   | 0.610086  |
| 1970-01-20 | 2.67815   | 0.614065  |
| 1970-01-21 |    NULL   |     NULL  |
| 1970-01-22 |    NULL   |     NULL  |
| 1970-01-23 |    NULL   |     NULL  |
 ...
| 2005-04-14 |  0.675824 | 0.0647169 |
| 2005-04-15 |      NULL |      NULL |
| 2005-04-16 |  0.574152 | 0.0925186 |
| 2005-04-17 |  0.462464 | 0.0726929 |
+------------+-----------+-----------+
12873 rows in set (1.14 sec)
```

3.2.2 Matlab

The database can be accessed directly from Matlab using a software[2] that works as an interface between Matlab and MySQL. From the Matlab command prompt the above queries are executed as:

```
% Connect to the database server.
mysql('open','rwc.lund.irf.se','isac','maunder');
% Select the isac database.
mysql('use isac');
% Load the data.
[t,mpsi,mwsi]=mysql('select * from mtwil_mag order by dt');
% Plot the data.
```

[2] http://solarwind.lund.irf.se/mysql/mysqlMatlab.html

```
plot(t,mpsi);
% Put date labels.
datetick;
```

3.2.3 Others

There are many other ways of accessing data from the database like Perl[3], PHP[4], Python[5], etc. We use the PhpMyAdmin[6] software to administer the database and various Perl scripts to add data to the database. PhpMyAdmin is web based and thus the database can be browsed by logging[7] in with the same user name and password as above.

[3] http://www.perl.org
[4] http://www.php.net/
[5] http://www.python.org/
[6] http://www.phpmyadmin.net/
[7] http://rwc.lund.irf.se/phpMyAdmin-2.6.2/

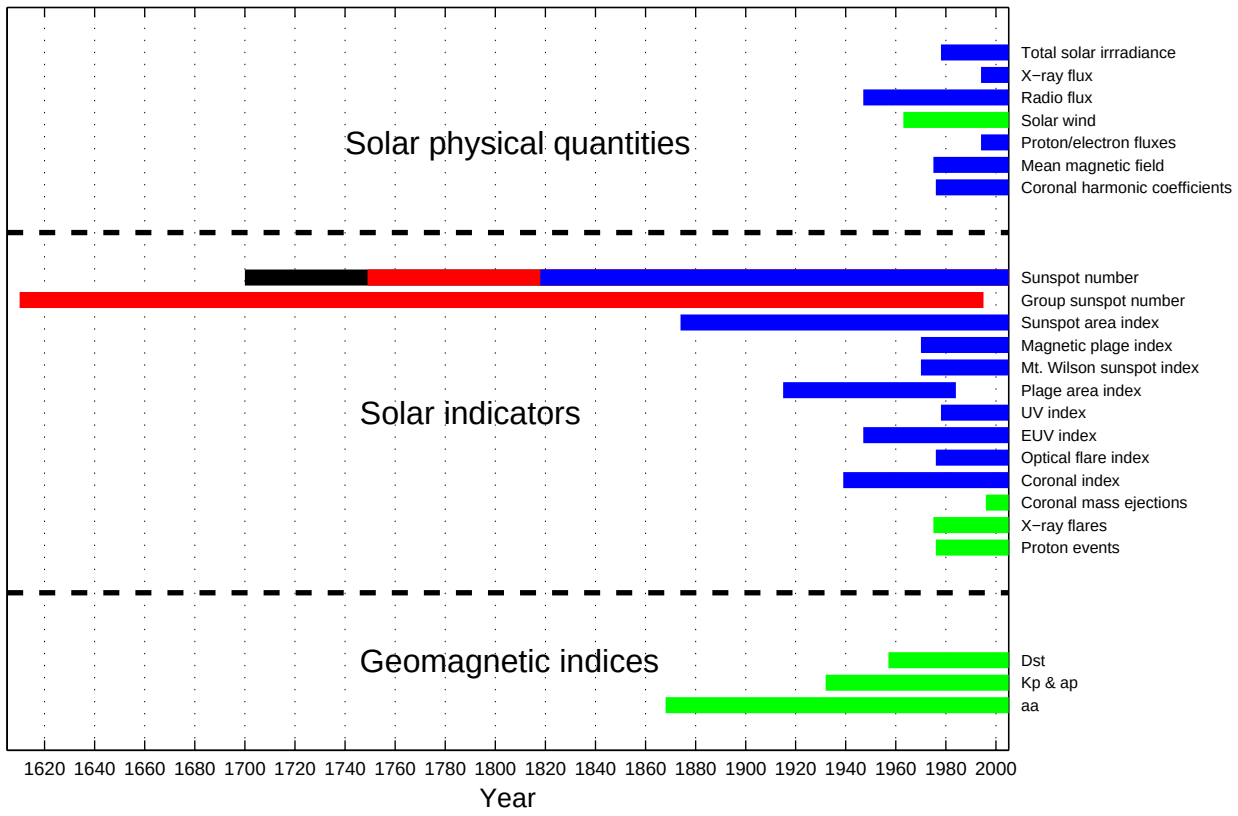

Figure 20: Timespans for solar data given in Table 4. Green, blue, red, and black bars for hourly, daily, monthly, and yearly values, respectively. The solar proxies are not included in this figure.

4 Conclusion

The purpose of this study is to identify data that permits quantification of climate variability due to variations in solar activity. In WP 100 a literary survey showed the time scales of solar variability, the processes behind solar variability, and how the Sun has been suggested to influence Earth's climate. In WP 201 we list data that can be used to study the solar influence on Earth's climate. Data were divided into solar physical quantities (SPQ) such as electromagnetic radiation and indicators such as indices and proxies. Physical quantities such as the solar radiation can be used directly as input to climate models. The sunspot number is an indicator of solar activity and can be used to derive a measure of solar output. The output could be any of the physical quantities. The advantage of an indicator such as the sunspot number or a proxy such as ^{14}C is the time period they span. After the indicator has been converted into a physical quantity, long time-series of the physical quantity can be obtained. Very long time-series are important for studies of non-anthropogenic influences on the climate.

All the data, retrievable from the database, are given in Table 4. In the table is also given the interval over which the data span, the delay time between the observation and availability, time resolution, and coverage. The time spans of the data are plotted in Figure 20. The time resolution is coded in different colours. The short period during which the SPQs have been measured is pronounced. The conversion from the indicators to the SPQs therefore plays a very important role

in order to enable long-term interpretations of the solar-climate coupling.

Solar physical quantities	**Interval**	**Delay**	**Res.**	**Cov.**
Total solar irradiance	1978 –	<6 m	daily	92.5%
X-ray flux	1994 –	0 d	daily	97.8%
Radio flux	1947 –	<30 d	daily	96.8%
Solar wind speed	1963 –	0 d	hourly	64.2%
Solar wind proton density	1963 –	0 d	hourly	59.9%
Interplanetary magnetic field	1963 –	0 d	hourly	65.1%
Proton fluxes	1994 –	0 d	daily	96.5%
Electron fluxes	1994 –	0 d	daily	97.6%
Mean magnetic field	1975 –	<40 d	daily	81.8%
Coronal harmonic coefficients	1976–	<60 d	daily	100%
Indicator: Indices	**Interval**	**Delay**	**Res.**	**Cov.**
Sunspot number	1818 –	<30 d	daily	95.3%
	1749 –	<40 d	monthly	100%
	1700 –	<400 d	yearly	100%
Group sunspot number	1610 - 1995	N/A	monthly	89.4%
Sunspot area index	1874 –	0 d	daily	100%
Magnetic plage index	1970 –	<10 d	daily	71.9%
Mt. Wilson sunspot index	1970 –	<10 d	daily	71.9%
Plage area index	1915 - 1984	N/A	daily	72.1%
Solar UV index	1978 –	0 d	daily	86.8%
Solar EUV index	1947 –	∼2 y	daily	100%
Optical flare index	1976 –	1-2 y	daily	100%
Coronal index	1939 –	∼2 y	daily	100%
Indicator: Proxies	**Interval**	**Delay**	**Res.**	**Cov.**
^{14}C, ^{10}Be concentrations	843 – 1982	N/A	5-10 yr	100%
	3 – 40 kyr B.P.	N/A	20-200 yr	100%
$\delta\,^{18}$O composition	0 – 123 kyr B.P.	N/A	50 yr	100%
Indicator: Lists	**Interval**	**Delay**	**Res.**	**Cov.**
Proton events	1976 –	<30 d	N/A	N/A
X-ray flares	1975 –	<30 d	N/A	N/A
Coronal mass ejections	1996 –	<5 m	N/A	N/A

Table 4: A summary of solar physical quantities and indicators electronically stored in the data base at the Swedish Institute of Space Physics. Solar wind parameters are available in real-time but the final values have a delay of 2-14 months. The Indicator/Lists are based on data/images with a temporal resolution of minutes to hours. Coronal harmonic coefficients are given for Carrington rotations but is calculated from daily magnetograms.

5 Appendix - ISAC data tables

Table name: **isgi_aa**		
Column name	Column type	Description
`dt`	`DATETIME`	The time stamp of the observation
`aa`	`INT`	aa index [nT]

Source: Two nearly antipodal magnetic observatories.

Procedure: The aa indices are derived using data from two nearly antipodal observatories, where magnetograms were available since 1868. For each three hour interval, K indices are measured at the two stations and converted back into amplitude; an individual aa index is the average of the northern and southern values, weighted to account for the small difference in latitude of the two stations, or for the slight changes in the very place of the observatory. The observatories used to derive aa are given in with weighting coefficients given in brackets.

Period	Observatory	Corr. Geomag. Lat.
	Northern Hemisphere	
1868-1925	Greenwich (1.007)	
1926-1956	Abinger (0.934)	
1957- ...	Hartland (1.059)	50.0°
	Southern Hemisphere	
1868-1919	Melbourne(0.967)	
1920-1979	Toolangui (1.033)	
1980- ...	Canberra (1.084)	45.2°

The aa index is in nanotesla (nT) and it represents the activity level at an invariant magnetic latitude of about 50°. The half-daily and daily mean values of aa are very close to the corresponding values of the am indices.

Coverage: 1 January 1868 - present

Resolution: 3 hours

Table name: **isgi_kp_ap**		
Column name	Column type	Description
`dt`	`DATETIME`	The time stamp of the observation
`kp`	`INT`	Kp index
`ap`	`INT`	ap index

Source: The subscript p means planetary and designates a global magnetic activity index. The following 13 observatories, which lie between 46 and 63 degrees north and south geomagnetic latitude, now contribute to the planetary indices: Lerwick (UK), Eskdalemuir (UK), Hartland (UK), Ottawa (Canada), Fredericksburg (USA), Meanook (Canada), Sitka (USA), Eyrewell (New Zealand), Canberra (Australia), Lovo (Sweden), Brorfelde (Denmark), Wingst and Niemegk (Germany).
Procedure: Ks indices isolate solar particle effects on the earth's magnetic field; over a 3-hour period, they classify into disturbance levels the range of variation of the more unsettled horizontal field component. Each activity level relates almost logarithmically to its corresponding disturbance amplitude. Three-hour indices discriminate conservatively between true magnetic field perturbations and the quiet-day variations produced by ionospheric currents. Ks indices range in 28 steps from 0 (quiet) to 9 (greatly disturbed) with fractional parts expressed in thirds of a unit. A Ks-value equal to 27, for example, means 2 and 2/3 or 3-; a Ks-value equal to 30 means 3 and 0/3 or 3 exactly; and a Ks-value equal to 33 means 3 and 1/3 or 3+. The arithmetic mean of the Ks values scaled at the 13 observatories listed above gives Kp.
The ap-index ranges from 0 to 400 and represents a Kp-value converted to a linear scale in nT (nanoTesla) - a scale that measures equivalent disturbance amplitude of a station at which K=9 has a lower limit of 400 nT.
Coverage: 1 January 1932 - present
Resolution: 3 hours

Table name: **mtwil_mag**		
Column name	Column type	Description
`dt`	`DATE`	The time stamp of the observation
`mpsi`	`FLOAT`	Magnetic Plage Strength Index (MPSI) [Gauss]
`mwsi`	`FLOAT`	Mt. Wilson Sunspot Index (MWSI) [Gauss]

Source: Magnetograms taken by the 150-foot Solar Tower at Mt. Wilson Observatory.
Procedure: For each magnetogram, an MPSI value and an MWSI value are calculated. To determine MPSI the sum of the absolute values of the magnetic field strengths for all pixels where the absolute value of the magnetic field strength is between 10 and 100 gauss is calculated. This number is then divided by the total of number of pixels (regardless of magnetic field strength) in the magnetogram. The MWSI values are determined in the same manner as the MPSI, though summation is only done for pixels where the absolute value of the magnetic field strength is greater than 100 gauss.
Coverage: January 19, 1970 - present
Resolution: daily values

Table name: **noaa_coronal**		
Column name	Column type	Description
`dt`	`DATE`	The time stamp of the observation
`ci`	`FLOAT`	Coronal Index (CI) [10^{16} W sr^{-1}]

Source: Data are calculated and provided by Dr. Voyto Rusin at the Astronomical Institute, Lomnicky Peak, Slovak Republic.
Procedure: The CI measures the total energy emitted by the Sun's outermost atmospheric layer (the corona) at a wavelength of 530.3 nm. It gives the radiant energy emitted by the entire visible corona within the Fe XIV spectral line. Daily means of irradiance intensities are computed from photometric patrol observations made at up to 8 ground-based stations. All line emissions have been converted with a linear transformation to a common intensity scale by shifting position angles of the measurements and by comparing values taken at all the sites.
Coverage: January 1, 1939 - present
Resolution: daily values

Table name: **noaa_dpd**		
Column name	Column type	Description
`dt`	`DATE`	The time stamp of the observation
`p1`	`FLOAT`	Proton flux with energy>1 MeV [protons cm^{-2} day^{-1} sr^{-1}]
`p10`	`FLOAT`	Proton flux with energy>10 MeV [protons cm^{-2} day^{-1} sr^{-1}]
`p100`	`FLOAT`	Proton flux with energy>100 MeV [protons cm^{-2} day^{-1} sr^{-1}]
`e06`	`FLOAT`	Electron flux with energy>0.6 MeV [electrons cm^{-2} day^{-1} sr^{-1}]
`e20`	`FLOAT`	Electron flux with energy>2 MeV [electrons cm^{-2} day^{-1} sr^{-1}]
`n`	`FLOAT`	Neutron monitor reading [% of background]

Source: Particle fluxes measured at geosynchronous altitudes by GOES spacecraft.
Procedure: N/A.
Coverage: January 1, 1994 - present
Resolution: daily values

Table name: **noaa_dsd**		
Column name	Column type	Description
`dt`	`DATE`	The time stamp of the observation
`m`	`FLOAT`	Multiplier corresponding to classification letters A,B,C,M,X
`v`	`FLOAT`	Value (v×m gives the X-ray background flux) [Wm^{-2}]

Source: The X-ray flux is measured by the primary GOES satellite.
Procedure: X-ray flux values below the B1 level can be erroneous. Energetic electron contamination of the x-ray sensors occurs. At times of high electron flux at geosynchronous altitude, the X-ray measurements in the low A-class range can be in error by 20-30%. Measurements taken during periods of low energetic electron fluxes are much more accurate.
Coverage: January 1, 1994 - present
Resolution: daily values

Table name: **noaa_dst**		
Column name	Column type	Description
`dt`	`DATETIME`	The time stamp of the observation
`dst`	`INT`	Dst index [nT]

Source:
Procedure: Dst (Disturbance Storm Time) equivalent equatorial magnetic disturbance indices are derived from hourly scalings of low-latitude horizontal magnetic variation. They show the effect of the globally symmetrical westward flowing high altitude equatorial ring current, which causes the "main phase" depression worldwide in the H-component field during large magnetic storms. This diskette contains the hourly indices for the period 1 Jan 1957 through 30 Sep 1992, as derived by M. Sugiura and T. Kamei, WDC-C2 for Geomagnetism, Faculty of Science, Kyoto Uni- versity, Kyoto 606, Japan.
Hourly H-component magnetic variations are analyzed to remove annual secular change trends from records of a worldwide array of low-latitude observatories. A cosine factor of the site latitude transforms residual variations to their equatorial equivalents and harmonic analysis isolates the term used as the Dst index. Sugiura described Dst derivation in ANNALS OF THE IGY.
Coverage: 1 January 1957 - present
Resolution: hourly values

Table name: **noaa_euv**		
Column name	Column type	Description
`dt`	`DATE`	The time stamp of the observation
`e107`	`FLOAT`	EUV proxy E10.7 [10^{22} $Wm^{-2}Hz^{-1}$]

Source: Data extracted by the empirical solar irradiance specification tool SOLAR2000.
Procedure: SOLAR2000 is designed to be a fundamental energy input into planetary atmosphere models, a comparative model with numerical first-principles solar models, and a tool to model or predict the solar radiation component of the space environment. SOLAR2000 includes a new EUV proxy, E10.7, which has the same units as the commonly used F10.7 cm solar radio flux. E10.7 can be used in existing models where F10.7 is traditionally used, but it offers significant improvement as an index of the energy input to the thermosphere and ionosphere.
Coverage: February 14, 1947 - present
Resolution: daily values

Table name: **noaa_flare**		
Column name	Column type	Description
`dt`	`DATE`	The time stamp of the observation
`n`	`FLOAT`	Daily flare index for northern hemisphere
`s`	`FLOAT`	Daily flare index for southern hemisphere
`tot`	`FLOAT`	Total daily flare index

Source: The Flare Index (FI) is determined by using the final grouped solar flares compiled by NGDC. FI data are produced by Dr. Tamer Atac and Dr. Atila Ozguc (both at Kandilli Observatory, Turkey).
Procedure: The FI is calculated for each flare using the formula $Q = i \times t$ where i is the importance coefficient of the flare reduced from its optical classification, and t is the duration of the flare in minutes. To obtain final daily values, the daily sums of the index for the northern and southern hemispheres and for the total surface are divided by the total time of observation of that day.
Coverage: January 1, 1976 - present
Resolution: daily values

Table name: **noaa_gssn**		
Column name	Column type	Description
`dt`	`DATE`	The time stamp of the observation
`num_days`	`INT`	Number of days to form the monthly means
`rg`	`FLOAT`	Monthly means of the group sunspot number R_g
`std`	`FLOAT`	Standard deviation of the means

Source: Drawings and white-light images of the Sun evaluated by Douglas Hoyt and Kenneth Schatten.
Procedure: R_g values were derived to provide a homogeneous record of solar activity from 1610 to 1995. Care was taken that the long-term changes are more self-consistent than are the changes using the Wolf Sunspot Numbers. The standard deviation represents the variability in the Group Sunspot Numbers and not their uncertainty.
Coverage: January, 1610 - December 1995
Resolution: monthly values

Table name: **noaa_iso_bard**		
Column name	Column type	Description
`dt`	`DATE`	The time stamp of the observation
`cnp`	`INT`	CNP [changes per mil. vs. present value]
`cnps`	`INT`	smoothed CNP [changes per mil. vs. present value]
`tsi25`	`FLOAT`	TSI scaled against MM TSI reductions of 25% [Wm^{-2}]
`tsi40`	`FLOAT`	TSI scaled against MM TSI reductions of 40% [Wm^{-2}]
`tsi55`	`FLOAT`	TSI scaled against MM TSI reductions of 55% [Wm^{-2}]
`tsi60`	`FLOAT`	TSI scaled against MM TSI reductions of 60% [Wm^{-2}]

Source: Bard, E., G. Raisbeck, F. Yiou, and J. Jouzel, Solar irradiance during the last 1200 years based on cosmogenic nuclides. TELLUS B 52(3), 985-992, 2000.
Procedure: Based on a quantitative study of the common fluctuations of ^{14}C and ^{10}Be production rates, we have derived a time series of the solar magnetic variability over the last 1200 years. This record is converted into irradiance variations by linear scaling based on previous studies of sun-like stars and of the Sun's behavior over the last few centuries. An accurate quantification of the climatic impact of this new irradiance record requires the use of coupled atmosphere-ocean general circulation models (GCMs). Total Solar Irradiance (TSI) with Maunder Minimum (MM) reductions of 25% - see Lean et al. 1995. TSI with MM reductions of 40%- see Zhang et al. 1994 and Solanki and Fligge, 1998. TSI with MM reductions of 55% - see Cliver et al. 1998. TSI with MM reductions of 60% - see Reid 1997.
Coverage: 843 - 1982
Resolution: semiannual values

Table name: **noaa_iso_gisp2**		
Column name	Column type	Description
`dtop`	`FLOAT`	Depth top
`dbot`	`FLOAT`	Depth bottom
`be`	`FLOAT`	^{10}Be concentration [10^3 atoms g^{-1}]
`bes`	`FLOAT`	Uncertainty in ^{10}Be concentration [10^3 atoms g^{-1}]
`agebot`	`INT`	Age bottom
`agetop`	`INT`	Age top

Source: Finkel, R.C., and K. Nishiizumi, Beryllium 10 concentrations in the Greenland Ice Sheet Project 2 ice core from 3-40 ka. Journal of Geophysical Research, vol. 102, 26,699-26,706, 1997.
Procedure: Melted water was collected from the outside of samples taken for cation and anion analysis by the UNH group. A small aliquot was taken for anion analysis (chloride, nitrate, and sulfate) and the remainder was weakly acidified with HNO_3 to yield a final pH of about 2. Be, Cl and Al carriers were then added. The Be (and Al and Cl) were concentrated from the melted ice using ion exchange resins. Be was then eluted from the cation exchange column, precipitated as $Be(OH)_2$ and ignited to BeO for accelerator mass spectrometry (AMS) measurement. The AMS measurements were carried out at the Lawrence Livermore National Laboratory Center for Accelerator Mass Spectrometry (Davis et al., 1990). The ^{10}Be (half-life $= 1.5 \times 10^6$ years) concentration was normalized to an ICN standard (diluted by K. Nishiizumi) after carrier blank and boron background correction.
Coverage: 3228 BP - 40,056 BP
Resolution: semidecadal values

Table name: **noaa_iso_ngrip**		
Column name	Column type	Description
`dt`	`DATE`	The time stamp of the observation, years before 2000 AD
`d18o`	`FLOAT`	δ^{18}O values [‰]

Source: North Greenland Ice Core Project members. 2004. High-resolution record of Northern Hemisphere climate extending into the last interglacial period, Nature, vol. 431, No. 7005, p. 147-151, 9 September 2004.
Procedure: High resolution Climate Record of the Northern Hemisphere back into the last Interglacial Period. The North Greenland Ice Core Project (NGRIP) site is located at 75.10°N and 42.32°W, elevation of 2,917 m, ice thickness of 3,085 m. The NGRIP drilling started in 1996, and bedrock was reached in July 2003. Here the NGRIP oxygen 18 values are listed as 50 year mean values using the same preliminary age scale as in Figure 2c of the accompanying paper. Data was measured against VSMOW at the Niels Bohr Institute for Astronomy, Physics and Geophysics, Department of Geophysics, University of Copenhagen. Accuracy of individual measurements is 0.07‰. The initial isotope data series is based on 5 cm continuous sampling from surface to bottom of the core, or 61,100 individual measurements.
Coverage: 0 - 122,950 BP
Resolution: 50-year values

Table name: **noaa_pevents**		
Column name	Column type	Description
`dts`	`DATETIME`	The time stamp of the observation, event start date
`dtm`	`DATETIME`	The time stamp of the observation, event maximum date
`prot`	`INT`	Proton flux [particles $cm^{-2}s^{-1}sr^{-1}$]
`cmeloc`	`CHAR(10)`	Associated CME, location
`cmedat`	`DATETIME`	Associated CME, onset time
`flrmax`	`DATETIME`	Associated flare, event maximum time
`flrimp`	`CHAR(2)`	Flare importance
`flropt`	`CHAR(2)`	Optical flare classification
`regloc`	`CHAR(15)`	Associated sunspot region, location)
`reg`	`INT`	Associated sunspot region number

Source: Particle fluxes are measured by GOES spacecraft at Geosynchronous orbit.
Procedure: Proton fluxes are integral 5-minute averages for energies > 10 MeV, given in Particle Flux Units (1 pfu = 1 particle $cm^{-2}s^{-1}sr^{-1}$), measured by GOES spacecraft at Geosynchronous orbit. SWO defines the start of a proton event to be the first of 3 consecutive data points with fluxes greater than or equal to 10 pfu. The end of an event is the last time the flux was greater than or equal to 10 pfu. This definition, motivated by SWO customer needs, allows multiple proton flares and/or interplanetary shock proton increases to occur within one SWO proton event. Additional data may be necessary to more completely resolve any individual proton event. Different detectors, onboard various GOES spacecraft, have taken the data since 1976. These proton data were processed using various algorithms. To date, no attempt has been made to cross-normalize the resulting proton fluxes. Flare associations are given, although data about individual Coronal Mass Ejections (CMEs), available from SOHO since 1996 only, are necessary to fully characterize each event.
Coverage: April 30, 1976 - present
Resolution: minute resolution

Table name: **noaa_plage**		
Column name	Column type	Description
`dt`	`DATE`	The time stamp of the observation
`area`	`FLOAT`	K-line Ca II plage area

Source: Daily solar chromospheric spectroheliograms obtained in the K-line of Ca II for the years 1915-1984 from Mt. Wilson Observatory were digitized and reduced by Dr. Peter Foukal, Cambridge Research and Instrumentation, Inc. (CRI) and his staff.
Procedure: The digitization was accomplished with an 800x490 CCD at an effective 512x512 format determined by an 8-bit frame grabber. The digitized images are stored on Exabyte tapes and are available to the scientific community. Each frame was viewed and the solar image centered. Software calculated the mean and root mean square of the pixel intensities within a rough polygon that enclosed the solar image. The software "painted" the plage pixels black, allowing the operator to check the software-chosen plage contour against the visual impression of the plage. The area of the plage was calculated as a fraction of the disc area, corrected for foreshortening, and expressed as a fraction of the solar hemisphere.
Coverage: August 6, 1915 - December 30, 1984
Resolution: daily values

Table name: **noaa_radio**		
Column name	Column type	Description
`dt`	`DATE`	The time stamp of the observation
`obs`	`FLOAT`	Observed 10.7cm radio flux [10^{-22} $Wm^{-2}Hz^{-1}$]
`adj`	`FLOAT`	Adjusted 10.7cm radion flux [10^{-22} $Wm^{-2}Hz^{-1}$]

Source: Daily measurements of F10.7 have been made by the National Research Council of Canada since 1947. Until May 31, 1991 the observations were made at the Algonquin Radio Observatory, near Ottawa. Over 1990-1991 the program was transferred to the Dominion Radio Astrophysical Observatory, near Penticton, British Columbia. From June 1, 1991, the data have originated from that location.
Procedure: Accurate spot determinations of the 10.7cm flux are made at local noon; previously 1700UT at Ottawa and now 2000UT at Penticton. The flux monitors have 1.8m paraboloidal antennas, which are equally sensitive to all points on the solar disc, and are equipped to measure emissions which are linearly-polarized in the North-South sense. In calculating the 10.7cm flux, the integrated emission from the solar disc at that wavelength is assumed to have no net linear polarization. The flux values are expressed in solar flux units (1 s.f.u. = 10^{-22} $Wm^{-2}Hz^{-1}$). The data are tabulated in two forms: the observed flux (obs), and the adjusted flux (adj). The former are the actual measured values, and are affected by the changing distance between the Earth and Sun throughout the year, whereas the latter are scaled to a standard distance of 1 AU. The observed flux values are useful in ionospheric physics and other terrestrial consequences of solar activity. The adjusted fluxes are more purely descriptive of the Sun's behaviour.
Coverage: February 14, 1947 - present
Resolution: daily values

Table name: **noaa_ssa**		
Column name	Column type	Description
`dt`	`DATE`	The time stamp of the observation
`tot`	`FLOAT`	Corrected total sunspot area [10^{-6} of hemisphere]
`north`	`FLOAT`	Corrected sunspot area for Northern Hemisphere [10^{-6} of hem.]
`south`	`FLOAT`	Corrected sunspot area for Southern Hemisphere [10^{-6} of hem.]

Source: The Royal Greenwich Observatory (RGO), US Air Force (USAF), and the US National Oceanic and Atmospheric Administration (NOAA).
Procedure: RGO compiled sunspot observations from a small network of observatories to produce a dataset of daily observations starting in May of 1874. The observatory concluded this dataset in 1976 after USAF started compiling data from its own Solar Optical Observing Network (SOON). This work was continued with the help of NOAA with much of the same information being compiled through to the present. Unfortunately, the more recent data is given in a different format from the original and there are definite changes in the reported parameters from the different sources. In an effort to append the RGO data with the more recent data the USAF and NOAA data have been reformatted to conform to the older RGO data format.
Coverage: May 9, 1874 - present
Resolution: daily values

Table name: **noaa_tsi_comp**		
Column name	Column type	Description
`dt`	`DATE`	The time stamp of the observation
`tsi`	`FLOAT`	Total Solar Irradiance (TSI) values, [Wm^{-2}]

Source: The TSI composite database was compiled from several different satellite TSI datasets by Claus Fröhlich and Judith Lean.
Procedure: The TSI data available here is based on six different satellite observations covering the period 1978 to present: 1) NIMBUS-7/HF, 2) Solar Maximum Mission (SMM) Active Cavity Radiometer Irradiance Monitor Experiment (ACRIM I), 3) The Earth Radiation Budget Satellite (ERBS), 4) The Upper Atmospheric Research Satellite (UARS) Active Cavity Radiometer Irradiance Monitor II Experiment (ACRIM II), 5) SOHO/VIRGO, and 6) ACRIM-Sat/ACRIM III. Adjustments are made for drifts in the radiometric data as described by Fröhlich and Lean, GRL, vol. 25, No. 23, 4377-4380, 1998. The absolute value of the composite is adjusted to the Space Absolute Radiometric Reference, which is considered to provide the most probable value to date of the absolute level of solar total irradiance.
Coverage: November 17, 1978 - present
Resolution: daily values

Table name: **noaa_uv**		
Column name	Column type	Description
`dt`	`DATE`	The time stamp of the observation
`mg2`	`FLOAT`	Mg II core-to-wing ratio
`source`	`INT`	Data source (see below)

Source: Prepared by the U.S. Dept. of Commerce, NOAA, Space Environment Center.
Procedure: The Mg II core-to-wing ratio is derived by taking the ratio of the h and k lines of the solar Mg II feature at 280 nm to the background or wings at approximately 278 nm and 282 nm. The h and k lines are variable chromospheric emissions while the background emissions are more stable. The result is a robust measure of chromospheric activity. This ratio has been shown to be a good measure of solar UV and EUV emissions. The data set was scaled to the original NOAA TIROS NOAA 9 data set with a linear fit of the overlapping data. The nature of the Mg II core-to-wing ratio and the quality of the data resulted in linear correlation coefficients between 0.98 and 0.999. Data source for the observations are: NaN - No data; 1 - NOAA TIROS and NOAA 9; 2 - NOAA 11; 3 - NOAA 9 (Alternate Algorithm); 4 - UARS SOLSTICE; 5 - GOME Data; 6 - NOAA 16.
Coverage: November 7, 1978 - present
Resolution: daily values

Table name: **noaa_xraylist**		
Column name	Column type	Description
`start`	`DATETIME`	Flare event start time
`end`	`DATETIME`	Flare event end time
`max`	`DATETIME`	Flare event max time
`lat`	`CHAR(3)`	Event latutude
`long`	`CHAR(3)`	Event longitude
`opt`	`CHAR(2)`	Optical flare importance (S,1,2,3) and brightness (F,N,B)
`xray`	`CHAR(5)`	X-ray class (C,M,X) and intensity
`flux`	`FLOAT`	Integrated flux for full event [Jm^{-2}]
`region`	`INT`	NOAA/USAF sunspot region number
`cmp`	`DATE`	Central meridian passage

Source: X-ray flare events observed at geosynchronous altitudes by GOES spacecraft.
Procedure: X-ray classes are classified according to the order of magnitude of the peak burst intensity I measured at the Earth by satellites in the 0.1 to 0.8 nm band as follows: Class B: $I < 10^{-6}$ Wm^{-2}; Class C: $10^{-6} \leq I < 10^{-5}$ Wm^{-2}; Class M: $10^{-5} \leq I < 10^{-4}$ Wm^{-2}; Class X: $I \geq 10^{-4}$ Wm^{-2}. X-ray flare events from 1975 have been cataloged using measurements made by GOES satellites. The GOES X-ray sensors operate on the ion-chamber principle: measured ion-chamber electric currents is proportional to the net ionization rate caused by incident X-ray flux on encapsulated noble gases. The current is proportional to the volume and density of the emitting plasma.
Coverage: September 1, 1975 - present
Resolution: minute resolution

Table name: **omni_2**		
Column name	Column type	Description
`dt`	`DATETIME`	The time stamp of the observation
`bz_gsm`	`FLOAT`	Solar wind B_z component in GSM [nT]
`n`	`FLOAT`	Solar wind particle density [cm^{-3}]
`v`	`FLOAT`	Solar wind speed [km s^{-1}]

Source: The OMNI 2 data set was created at NSSDC in 2003 as a successor to the OMNI data set first created in the mid-1970's.
Procedure: The OMNI 2 data set contains hourly resolution solar wind magnetic field and plasma data from several spacecraft in geocentric orbit and in orbit about the L1 Lagrange point approximately $225R_E$ in front of the Earth.
Coverage: November 27, 1963 - present
Resolution: hourly values

Table name: **sdac_cme**		
Column name	Column type	Description
`dt`	`DATETIME`	The time stamp of the observation
`pa`	`INT`	Central PA [degrees]
`width`	`INT`	Angular width [degrees]
`speed_lin`	`INT`	Linear speed [km s^{-1}]
`speed_2_i`	`INT`	2nd order speed, initial [km s^{-1}]
`speed_2_f`	`INT`	2nd order speed, fina [km s^{-1}]l
`speed_2_20r`	`INT`	2nd order speed, $20R_\odot$ [km s^{-1}]
`acc`	`FLOAT`	Acceleration [m s^{-2}]
`mpa`	`INT`	Measurement PA [degrees]
`remark`	`CHAR(80)`	Remarks

Source: This CME catalog is generated and maintained by NASA and The Catholic University of America in cooperation with the Naval Research Laboratory.
Procedure: CME heights are measured at the fastest segment of the leading edge with respect to the disk center. Numbers in 2nd order fit columns correspond to the speed at the last height of measurement and at a distance of 20 solar radii. Central Position Angle measured from Solar North in degrees (Counter clockwise).
Coverage: January 1, 1996 - present
Resolution: second resolution

Table name: **sidc_ssn_y**		
Column name	Column type	Description
`dt`	`DATE`	The time stamp of the observation
`ssn`	`FLOAT`	Yearly sunspot number
Table name: `sidc_ssn_m`		
Column name	Column type	Description
`dt`	`DATE`	The time stamp of the observation
`ssn`	`FLOAT`	Monthly sunspot number
Table name: `sidc_ssn_d`		
Column name	Column type	Description
`dt`	`DATE`	The time stamp of the observation
`ssn`	`INT`	Daily sunspot number

Source: The sunspot number is evaluated by Solar Influences Data analysis Center, Regional Warning Center Belgium, World Data Center for the Sunspot Index, Royal Observatory of Belgium.

Procedure: An observer computes a daily sunspot number by multiplying the number of groups he sees by ten and then adding this product to his total count of individual spots. Results, however, vary greatly, since the measurement strongly depends on observer interpretation and experience and on the stability of the Earth's atmosphere above the observing site. Moreover, the use of Earth as a platform from which to record these numbers contributes to their variability, too, because the sun rotates and the evolving spot groups are distributed unevenly across solar longitudes. To compensate for these limitations, each daily international number is computed as a weighted average of measurements made from a network of cooperating observatories.

Coverage: 1700 - present (yearly); January 1749 - present (monthly); January 1, 1818 - present (daily)

Resolution: yearly, monthly, and daily values

Table name: **wso_gfhc**		
Column name	Column type	Description
dt	DATE	The time stamp of the observation
g00	FLOAT	Spherical harmonic coefficient $g_{0,0}$ [Gauss]
g10	FLOAT	Spherical harmonic coefficient $g_{1,0}$ [Gauss]
g11	FLOAT	Spherical harmonic coefficient $g_{1,1}$ [Gauss]
g20	FLOAT	Spherical harmonic coefficient $g_{2,0}$ [Gauss]
g21	FLOAT	Spherical harmonic coefficient $g_{2,1}$ [Gauss]
g22	FLOAT	Spherical harmonic coefficient $g_{2,2}$ [Gauss]
⋮	⋮	⋮
g97	FLOAT	Spherical harmonic coefficient $g_{9,7}$ [Gauss]
g98	FLOAT	Spherical harmonic coefficient $g_{9,8}$ [Gauss]
g99	FLOAT	Spherical harmonic coefficient $g_{9,9}$ [Gauss]
h11	FLOAT	Spherical harmonic coefficient $h_{1,1}$ [Gauss]
h21	FLOAT	Spherical harmonic coefficient $h_{2,1}$ [Gauss]
h22	FLOAT	Spherical harmonic coefficient $h_{2,2}$ [Gauss]
⋮	⋮	⋮
h97	FLOAT	Spherical harmonic coefficient $h_{9,7}$ [Gauss]
h98	FLOAT	Spherical harmonic coefficient $h_{9,8}$ [Gauss]
h99	FLOAT	Spherical harmonic coefficient $h_{9,9}$ [Gauss]

Source: Magnetograms obtained at Wilcox Solar Observatory, Stanford University.
Procedure: The coronal magnetic field is calculated from photospheric field observations with a potential field model. The field is forced to be radial at the source surface to approximate the effect of the accelerating solar wind on the field configuration. This "classic" computation locates the source surface at 2.5 solar radii, assumes that the photospheric field has a meridional component and requires a somewhat ad hoc polar field correction to closely match the observations of the IMF at Earth.
Coverage: Carrington rotation 1642 - present
Resolution: Carrington rotations

Table name: **wso_smmf**		
Column name	Column type	Description
dt	DATE	The time stamp of the observation
mf	INT	Solar mean magnetic field [μT]

Source: SMMF obtained using magnetograph at Wilcox Solar Observatory, Stanford University.
Procedure: SMMF values are obtained from the Zeeman splitting in the Fe I line at 5250Å from three-minute integrations repeated severela times each day. The final daily SMMF value is computed as a weighted average of the individual observations, with a standard deviation around 0.05 G.
Coverage: May 16, 1975 - present
Resolution: daily values

References

Ataç, T., and A. Özgüç, Flare index of solar cycle 22, *Solar Physics*, *180*, 397–407, 1998.

Ballester, J. L., R. Oliver, and M. Carbonell, Return of the near 160 day periodicity in the photospheric magnetic flux during solar cycle 23, *The Astrophysical Journal*, *615*, L173–L176, 2004.

Bard, E., G. Raisbeck, F. Yiou, and J. Jouzel, Solar irradiance during the last 1200 years based on cosmogenic nuclides, *Tellus*, *52B*, 985–992, 2000.

Bartels, J., The standardized index, ks, and the planetary index kp, *IATME Bull.*, *97*(12b), 1949.

Beer, J., A. Blinov, G. Bonani, R. C. Finkel, H. J. Hofmann, B. Lehmann, H. Oeschger, A. Sigg, J. Schwander, T. Staffelbach, B. Stauffer, M. Suter, and W. Wölfli, Use of ^{10}Be in polar ice to trace the 11-year cycle of solar activty, *Nature*, *347*, 164–166, 1990.

Boberg, F., H. Lundstedt, J. T. Hoeksema, P. H. Scherrer, and W. Lui, Solar mean magnetic field variability: A wavelet approach to WSO and SOHO/MDI observations, *Journal of Geophysical Research*, *107*(A10), doi:10.1029/2001JA009195, 2002.

Cebula, R. P., M. T. DeLand, and B. M. Schlesinger, Estimates of solar variability using the Solar Backscatter Ultraviolet (SBUV) 2 Mg II index from the NOAA 9 satellite, *Journal of Geophysical Research*, *97*(D11), 11,613–11,620, 1992.

Cebula, R. P., M. T. DeLand, and E. Hilsenrath, NOAA 11 solar backscattered ultraviolet, model 2 (SBUV/2) instrument solar spectral irradiance measurements in 1989-1994 1. Observations and long-term calibration, *Journal of Geophysical Research*, *103*(D13), 16,235–16,249, 1998.

Covington, A. E., Solar radio emission at 10.7 cm, 1947-1968, *Journal of the Royal Astronomical Society of Canada*, *63*(3), 125–132, 1969.

DeLand, M. T., and R. P. Cebula, Composite Mg II solar activity index for solar cycles 21 and 22, *Journal of Geophysical Research*, *98*(D7), 12,809–12,823, 1993.

DuBois, P., MySQL - The definitive quide to using, programming, and administering MySQL 4, *Sams Developer's Library*, p. 1248, 2003.

Finkel, R. C., and K. Nishiizumi, Beryllium 10 concentrations in the Greenland Ice Sheet Project 2 ice core from 3-40 ka, *Journal of Geophysical Research*, *102*(C12), 26,699–26,706, 1997.

Fligge, M., S. K. Solanki, and Y. C. Unruh, Modelling irradiance variations from the surface distribution of the solar magnetic field, *Astronomy & Astrophysics*, *353*, 380–388, 2000.

Foukal, P., The behavior of solar magnetic plages measured from Mt. Wilson observatories between 1915-1984, *Geophysical Research Letters*, *23*(16), 2169–2172, 1996.

Fröhlich, C., and J. Lean, The Sun's total irradiance: Cycles, trends and related climate change uncertainties since 1976, *Geophysical Research Letters*, *25*(23), 4377–4380, 1998.

Fröhlich, C., D. A. Crommelynck, C. Wehrli, M. Anklin, S. Dewitte, A. Fichot, W. Finsterle, A. Jiménez, A. Chevalier, and H. Roth, In-flight performances of the VIRGO solar irradiance instruments on SOHO, *Solar Physics*, *175*, 267–286, 1997.

Garcia, H. A., Temperature and emission measure from GOES soft X-ray measurements, *Solar Physics*, *154*, 275–308, 1994.

García, R. A., P. Boumier, J. Charra, T. Foglizzo, A. H. Gabriel, G. Grec, C. Régulo, J. M. Robillot, S. Turck-Chièze, and R. K. Ulrich, The integrated magnetic field of the Sun as seen by GOLF on board SOHO, *Astronomy & Astrophysics*, *346*, 626–632, 1999.

Gosling, J. T., Coronal mass ejections: An overview, *AGU Geophysical Monograph 99*, pp. 9–16, 1997.

Győri, L., Automation of area measurements of sunspots, *Solar Physics*, *180*, 109–130, 1998.

Harvey, J., and the GONG Team, GONG instrument and science, *The Bulletin of the Astronomical Society of India*, *26*, 135–142, 1998.

Hoyt, D. V., and K. H. Schatten, A new look at Wolf sunspot numbers in the late 1700's, *Solar Physics*, *138*, 387–397, 1992.

Hoyt, D. V., and K. H. Schatten, Group sunspot numbers: A new solar activity reconstruction, *Solar Physics*, *181*(2), 491–512, 1998.

Hoyt, D. V., H. L. Kyle, J. R. Hickey, and R. H. Maschhoff, The Nimbus 7 solar total irradiance: A new algorithm for its derivation, *Journal of Geophysical Research*, *97*(A1), 51–63, 1992.

Ipavich, F. M., A. B. Galvin, S. E. Lasley, J. A. Paquette, S. Hefti, K. Reiche, M. A. Coplan, G. Gloeckler, P. Bochsler, D. Hovestadt, H. Grünwaldt, M. Hilchenbach, and 17 more, Solar wind measurements with SOHO: The CELIAS/MTOF proton monitor, *Journal of Geophysical Research*, *103*(A8), 17,205–17,213, 1998.

Kotov, V. A., and A. B. Severny, Mean magnetic field of the Sun as a star. Catalogue 1968-1976, *Soviet Geophysical Committee, Academy of Sciences of the USSR*, pp. 1–24, 1983.

Kotov, V. A., P. H. Scherrer, R. F. Howard, and V. I. Haneychuk, Magnetic field of the Sun as a star: The Mount Wilson Observatory catalog 1970-1982, *The Astrophysical Journal Supplement Series*, *116*, 103–117, 1998.

Lean, J., Solar ultraviolet irradiance variations: A review, *Journal of Geophysical Research*, *92*(D1), 839–868, 1987.

Lee III, R. B., B. R. Barkstrom, and R. D. Cess, Characteristics of the earth radiation budget experiment solar monitors, *Applied Optics*, *26*(15), 3090–3096, 1987.

Lee III, R. B., M. A. Gibson, R. S. Wilson, and S. Thomas, Long-term total solar irradiance variability during sunspot cycle 22, *Journal of Geophysical Research*, *100*(A2), 1667–1675, 1995.

Lepping, R. P., M. H. Acuña, L. F. Burlaga, W. M. Farrell, J. A. Slavin, K. H. Schatten, F. Mariani, N. F. Ness, F. M. Neubauer, Y. C. Whang, J. B. Byrnes, R. S. Kennon, P. V. Panetta, J. Scheifele, and E. M. Worle, The WIND magnetic field investigation, *Space Science Reviews*, *71*, 207–229, 1995.

Luhmann, J. G., CMEs and space weather, *AGU Geophysical Monograph 99*, pp. 291–299, 1997.

Mayaud, P. N., Derivation, meaning, and use of geomagnetic indices, *Geophysical Monograph Series,* American Geophysical Union, 1980.

McComas, D. J., S. J. Bame, P. Barker, W. C. Feldman, J. L. Phillips, P. Riley, and J. W. Griffee, Solar wind electron proton alpha monitor (SWEPAM) for the Advanced Composition Explorer, *Space Science Reviews*, *86*, 563–612, 1998.

Muscheler, R., J. Beer, and B. Kromer, Long-term climate variations and solar effects, in *Solar variability as an input to the Earths environment. International Solar Cycle Studies Symposium*, edited by A. Wilson, pp. 305–316, ESA SP-535, Noordwijk, 2003.

Ness, N. F., C. S. Scearce, and J. B. Seek, Initial results of the Imp 1 magnetic field experiment, *Journal of Geophysical Research*, *69*(17), 3531–3569, 1964.

North Greenland Ice Core Project members, High-resolution record of Northern Hemisphere climate extending into the last interglacial period, *Nature*, *431*(7005), 147–151, 2004.

Ogilvie, K. W., M. A. Coplan, P. Bochsler, and J. Geiss, Solar wind observations with the ion composition instrument aboard the ISEE-3/ICE spacecraft, *Solar Physics*, *124*(1), 167–183, 1989.

Ogilvie, K. W., D. J. Chornay, R. J. Fritzenreiter, F. Hunsaker, J. Keller, J. Lobell, G. Miller, J. D. Scudder, E. C. Sittler, Jr., R. B. Torbert, D. Bodet, G. Needell, A. J. Lazarus, and 4 more, SWE, a comprehensive plasma instrument for the WIND spacecraft, *Space Science Reviews*, *71*, 55–77, 1995.

Onsager, T. G., R. Grubb, J. Kunches, L. Matheson, D. Speich, R. Zwickl, and H. Sauer, Operational uses of the GOES energetic particle detectors, *SPIE Conference Proceedings*, *2812*, 281–290, 1996.

Parker, D. G., J. M. Pap, R. K. Ulrich, L. E. Floyd, and D. K. Prinz, Developing new Mount Wilson magnetic indices to model solar UV variations, *Bulletin of the American Astronomical Society*, *29*(2), 902–903, 1997.

Paularena, K. I., J. D. Richardson, A. J. Lazarus, G. N. Zastenker, and P. A. Dalin, IMP-8, WIND and INTERBALL observations of the solar wind, *Physics and Chemistry of the Earth*, *22*(7-8), 629–637, 1997.

Rottman, G., Variations of solar ultraviolet irradiance observed by the UARS SOLSTICE - 1991 to 1999, *Space Science Reviews*, *94*, 83–91, 2000.

Rybanský, M., V. Rušin, P. Gašpar, and R. C. Altlock, Coronal index of solar activity VII, years 1988-1991, *Solar Physics*, *152*, 487–495, 1994a.

Rybanský, M., V. Rušin, M. Minarovjech, and P. Gašpar, Coronal index of solar activity: Years 1939-1963, *Solar Physics*, *152*, 153–159, 1994b.

Scherrer, P. H., J. M. Wilcox, L. Svalgaard, T. L. Duvall, Jr., P. H. Dittmer, and E. K. Gustafson, The mean magnetic field of the Sun: Observations at Stanford, *Solar Physics*, *54*, 353–361, 1977.

Scherrer, P. H., R. S. Bogart, R. I. Rush, J. T. Hoeksema, A. G. Kosovichev, J. Schou, W. Rosenberg, L. Springer, T. D. Tarbell, A. Title, C. J. Wolfson, I. Zayer, and the MDI engineering team, The Solar Oscillations Investigation – Michelson Doppler Imager, *Solar Physics*, *162*, 129–188, 1995.

Smith, C. W., J. L'Heureux, N. F. Ness, M. H. Acuña, L. F. Burlaga, and J. Scheifele, The ACE magnetic fields experiment, *Space Science Reviews*, *86*, 613–632, 1998.

St. Cyr, O. C., R. A. Howard, N. R. Sheeley, Jr., S. P. Plunkett, D. J. Michels, S. E. Paswaters, M. J. Koomen, G. M. Simnett, B. J. Thompson, J. B. Gurman, R. Schwenn, D. F. Webb, E. Hildner, and P. L. Lamy, Properties of coronal mass ejections: SOHO LASCO observations from January 1996 to June 1998, *Journal of Geophysical Research*, *105*(A8), 18,169–18,185, 2000.

Steinegger, M., M. Vázquez, J. A. Bonet, and P. N. Brandt, On the energy balance of solar active regions, *The Astrophysical Journal*, *461*, 478–498, 1996.

Stuiver, M., P. J. Reimer, E. Bard, J. W. Beck, G. S. Burr, K. A. Hughen, B. Kromer, G. McCormac, J. Van der Plicht, and M. Spurk, INTCAL98 radiocarbon age calibration, 24,000-0 cal BP, *Radiocarbon*, *40*(3), 1041–1083, 1998.

Sugiura, M., Hourly values of equatorial *Dst* for the IGY, *Annals of the International Geophysical Year*, *35*, 9–45, 1964.

Tobiska, W. K., Validating the solar EUV proxy, $E_{10.7}$, *Journal of Geophysical Research*, *106*(A12), 29,969–29,978, 2001.

Usoskin, I. G., S. K. Solanki, M. Schüssler, K. Mursula, and K. Alanko, Millenium-scale sunspot number reconstruction: Evidence for an unusually active Sun since the 1940s, *Physical Review Letters*, *91*(21), 211,101–1–211,101–4, 2003.

Viereck, R. A., and L. C. Puga, The NOAA Mg II core-to-wing solar index: Construction of a 20-year time series of chromospheric variability from multiple satellites, *Journal of Geophysical Research*, *104*(A5), 9995–10,005, 1999.

Waldmeier, M., The sunspot-activity in the years 1610-1960, *Schulthess & Co. AG*, Zürich, 1961.

Willson, R. C., Measurements of solar total irradiance and its variability, *Space Science Reviews*, *38*, 203–242, 1984.

Willson, R. C., Irradiance observations of SMM, Spacelab 1, UARS, and ATLAS experiments, in *The Sun as a variable star, solar and stellar irradiance variations*, edited by J. Pap, C. Fröhlich, H. S. Hudson, and S. Solanki, pp. 54–62, Cambridge University Press, Cambridge UK, 1994.

Willson, R. C., The ACRIMSAT/ACRIM III experiment - Extending the precision, long-term total solar irradiance climate database, *The Earth Observer*, *13*, 14–17, 2001.

Woods, T. N., G. J. Rottman, and G. J. Ucker, Solar-stellar irradiance comparison experiment 1: 2. Instrument calibrations, *Journal of Geophysical Research*, *98*(D6), 10,679–10,694, 1993.

Zhao, X., and J. T. Hoeksema, Unique determination of model coronal magnetic fields using photospheric observations, *Solar Physics*, *143*, 41–48, 1993.